HHS Public Access

Author manuscript

Circ Res. Author manuscript; available in PMC 2019 October 01.

Published in final edited form as:

Circ Res. 2018 September 28; 123(8): 964–985. doi:10.1161/CIRCRESAHA.117.312576.

Mechanisms of Connexin-Related Lymphedema: A Critical Role for Cx45, but not Cx43 or Cx47, in the Entrainment of Spontaneous Lymphatic Contractions

Jorge A. Castorena-Gonzalez[1], **Scott D. Zawieja**[1], **Min Li**[1], **R. Sathish Srinivasan**[3], **Alexander M. Simon**[4], **Cor de Wit**[5], **Roger de la Torre**[2], **Luis A. Martinez-Lemus**[1], **Grant W. Hennig**[6], **Michael J. Davis**[1]

[1]Dept. of Medical Pharmacology and Physiology and University of Missouri School of Medicine

[2]Dept. of Medicine, University of Missouri School of Medicine

[3]Cardiovascular Biology Research Program, Oklahoma Medical Research Foundation, Oklahoma City OK

[4]Dept. of Physiology, University of Arizona, Tucson AZ

[5]Institute of Physiology, University of Luebeck, Luebeck Germany

[6]Dept. of Pharmacology, University of Vermont, Burlington VT

Abstract

Rationale: Mutations in *GJC2* and *GJA1*, encoding connexins (Cxs) 47 and 43 respectively, are linked to lymphedema, but the underlying mechanisms are unknown. Because efficient lymph transport relies on the coordinated contractions of lymphatic muscle cells (LMCs) and the electrical coupling of those through Cxs, Cx-related lymphedema is proposed to result from dyssynchronous contractions of lymphatic vessels.

Objective: Determine which Cx isoforms in LMCs and/or lymphatic endothelial cells (LECs) are required for the entrainment of lymphatic contraction waves and efficient lymph transport.

Methods and Results: We developed novel methods to quantify the spatiotemporal entrainment of lymphatic contraction waves and used optogenetic techniques to analyze calcium signaling within and between the LMC and LEC layers. Genetic deletion of the major LEC Cxs (Cx43, Cx47, or Cx37) revealed that none were necessary for the synchronization of the global calcium events that triggered propagating contraction waves. We identified Cx45 in human and mouse LMCs as the critical Cx mediating the conduction of pacemaking signals and entrained contractions. Smooth muscle-specific Cx45 deficiency resulted in 10–18-fold reduction in conduction speed, partial-to-severe loss of contractile coordination, and impaired lymph pump function ex vivo and in vivo. Cx45-deficiency resulted in profound inhibition of lymph transport in vivo, but only under an imposed gravitational load.

Address correspondence to: Dr. Michael J. Davis, Department of Medical Pharmacology and Physiology, One Hospital Drive, MA415 Medical Sciences Building, University of Missouri, Columbia, MO 65212, Tel: 573-884-5181, Fax: 573-884-4276 davismj@health.missouri.edu.

Conclusions: Our results: 1) identify Cx45 as the Cx isoform mediating the entrainment of the contraction waves in LMCs; 2) show that major endothelial Cxs are dispensable for the entrainment of contractions; 3) reveal a lack of coupling between LECs and LMCs, in contrast to arterioles; 4) point to lymphatic valve defects, rather than contraction dyssynchrony, as the mechanism underlying *GJC2*- or *GJA1*-related lymphedema; and 5) show that a gravitational load exacerbates lymphatic contractile defects in the intact mouse hindlimb, which is likely critical for the development of lymphedema in the adult mouse.

Keywords

Lymphatic system; connexin; lymphedema; calcium signaling; smooth muscle contraction; in vivo imaging; lymph; vascular disease; contraction; lymphatic smooth muscle; lymphatic endothelium

Keywords

Physiology; Vascular Biology; Vascular Disease

INTRODUCTION

Recent genetic screens reveal that patients with inherited mutations in certain gap junction proteins, connexins (Cxs), develop primary lymphedema; however, the underlying mechanisms are not clear. Two independent groups have identified missense mutations in *GJC2* (Cx47) in patients with primary lymphedema, as characterized by fluid and protein accumulation in their dependent extremities [1, 2]. Also, women with *GJC2* mutations exhibit a higher incidence of breast cancer-related secondary lymphedema in their extremities [3]. Subsequent to these studies, Brice et al. [4] identified primary lymphedema in three generations of a family with a mutation in another Cx, *GJA1* (Cx43). Although *Gjc2* and *Gja1* deficiencies are known to cause developmental lymphatic valve abnormalities in mice [5–7], so do deficiencies in *Gja4* (Cx37), another Cx expressed along with *Gjc2* and *Gja1* in lymphatic endothelium. However, *GJA4* mutations have not been identified in human patients nor linked to lymphedema, nor have lymphatic valve abnormalities been documented in any human patients with Cx-related lymphedema. An alternative explanation for Cx-related lymphedema was suggested by the authors of recent clinical and genetic studies [1-4]: that Cx mutations produce deficits in contraction coordination due to impaired gap junction communication in mature lymphatic vessels [1, 3, 4]. This idea is not without precedent because lymphatic contractile dysfunction is also thought to contribute to acquired forms of lymphedema [8–11] and to other diseases that have a lymphatic component [12–15], including congestive heart failure [15–17], obesity [18, 19], and peripheral artery/venous disease [13, 20].

How might mutations or deficiencies in vascular Cxs lead to lymphatic contractile dysfunction? In many regions of the body, lymph transport must be accomplished against hydrostatic pressure gradients [21, 22] that arise from the imposition of gravitational loads [23, 24]. Consequently, efficient lymph propulsion relies critically on the intrinsic spontaneous contractions of lymphatic smooth muscle cells (LMCs), in conjunction with one-way lymphatic valves that minimize lymph backflow [25–27]. The contraction of all LMCs within a

pumping unit, the lymphangion, must be coordinated to efficiently propel lymph downstream into the next segment [28] and ultimately into the central veins through the lymphovenous valves [5, 29]. LMC contractions are rapid, transient, large-amplitude events [30] initiated by action potentials (APs) that originate at a pacemaking site within the lymphatic vessel wall and then rapidly propagate from cell to cell along the vessel. Electrical coupling between adjacent cells in lymphatic vessels, as well as blood vessels, is thought to be mediated entirely by Cxs.

Cxs are a family of proteins that assemble into 6-unit connexons, or hemichannels, that dock together on adjacent cells to form gap junction intercellular channels, allowing for direct electrical coupling and transfer of small molecules [31–34]. The Cx family is composed of 21 different isoforms in humans and 20 in mice [31, 32, 35]. Mutations in 10 different Cx isoforms are linked to over twenty different genetic diseases in humans [36, 37]. Cx37 and Cx43, along with Cx40 (*Gja5*), are expressed in blood vascular endothelium [38–40] where they mediate conducted hyperpolarization — a fundamental property of microvascular networks whereby local dilator stimuli can spread upstream to recruit larger vessels [41, 42]. Cxs in the arterial smooth muscle layer have less defined roles but presumably mediate the conduction of depolarizing signals, where the spread is severely limited in comparison to conduction in the endothelium [43–45]. The smooth muscle and endothelial cell layers in blood vessels are coupled structurally by myoendothelial gap junctions (MEGJs) so that electrical signals (and to a lesser extent second messengers) can pass between the two layers. Changes in the expression and/or phosphorylation state [46, 47] of blood vascular Cxs have been linked to various cardiovascular pathologies including hypertension [48–50] and ischemia/reperfusion injury [51, 52].

Much less is known about the roles of connexins in LMCs and lymphatic endothelial cells (LECs). Three previous studies used pharmacological inhibitors of gap junctions to provide evidence that electrical coupling between cells in the lymphatic wall is required for the synchronization of contractile waves in lymphatic vessels in vivo [53–55]. Unfortunately, those inhibitors were not specific for any particular Cx isoform(s) and are now known to have off-target effects on ion channels that could affect smooth muscle contraction directly. Thus, the specific Cx isoforms expressed in LMCs and their physiological roles are unknown, nor it is clear whether the electrical signals required to trigger lymphatic contraction waves are conducted along the smooth muscle or endothelial layers, or both. Are Cxs in lymphatic endothelium important for the conduction of electrical signals in the lymphatic wall, as in arterioles? LEC Cxs are known to be critical for lymphatic and venous valve development [6, 37, 56, 57] and possibly for shear stress sensing by lymphatic endothelium [58–60]. In mice, combined haplodeficiency of Cx43 ($Cx43^{+/-}$) with either $Cx37^{-/-}$ or $Cx37^{+/-}$ mice results in the development of fewer lymphatic valves, while complete Cx43 deficiency or combined Cx37 deletion and Cx43 deficiency leads to chylothorax and nuchal edema due to both fewer and abnormal valves [6, 35, 57]. It remains uncertain whether lymphatic valve defects or conduction abnormalities account for Cx-related lymphedema, but this idea cannot be tested in human patients with currently available methods.

For this reason, we utilized mouse models to test the hypothesis that lymphatic vessels deficient in either of the three known LEC Cx isoforms, Cx43, Cx47 or Cx37, result in

deficits in lymphatic contraction coordination due to impaired gap junctional communication. Surprisingly, our results indicated that all three LEC Cxs are dispensable for the initiation and propagation of lymphatic contraction waves. We then identified the Cx isoforms expressed in the lymphatic smooth muscle layer, confirmed our findings in human lymphatics, and generated new mouse models to investigate the consequences of smooth-muscle specific Cx deletion. We found that Cx45 is the critical, and perhaps the only, Cx isoform required for entrainment of lymphatic contraction waves. The use of optogenetic techniques to study conducted and non-conducted LMC- and LEC-specific calcium signals confirmed that the two layers are functionally uncoupled in healthy lymphatic vessels. Cx45 deficiency resulted in profound inhibition of lymph transport in vivo, but only under an imposed gravitational load. Our results therefore point to developmental lymphatic valve defects as the underlying cause of Cx-related lymphedema in human patients and show that Cx-related defects in the mouse require the imposition of a gravitational load before the subsequent development of lymphedema.

METHODS

The authors declare that all data that support the findings of this study are available within the article and its Online Supplementary files. Detailed methods for all the experimental protocols and techniques, mouse strains, data/image processing and analysis, and relevant references are provided in the *Online Data Supplement*.

RESULTS

Cxs normally expressed in the lymphatic endothelium are dispensable for the initiation, coordination, and propagation of lymphatic contraction waves.

We used mouse popliteal afferent lymphatic vessels as an experimental model. Like lymphatics from the periphery of humans, these vessels exhibit strong contractions to propel lymph centrally, often against a substantial adverse pressure gradient [10]. We first tested whether the Cx isoforms previously detected in mouse mesentery and/or thoracic duct were also present in popliteal afferent lymphatic vessels. For reasons that are not completely clear, lymphatic collectors from the visceral cavity of the mouse do not exhibit propulsive contractions [61], unlike all other species studied, making them poor models for contractile studies. Immunofluorescence imaging of popliteal lymphatic tissue sections and whole-mounts showed expression of Cx43 and Cx37 exclusively in the endothelial cell layer. At valves, Cx43 was preferentially expressed on the upstream face of valve leaflets and Cx37 was preferentially distributed on the downstream face (Online Figure I), consistent with previous descriptions of lymphatics in other regions [6]. Also consistent with previous studies [6, 56], $Cx37^{-/-}$ popliteal lymphatics had fewer valves and significantly longer distances between valves (3.3±0.6 mm for $Cx37^{-/-}$ vessels compared to 1.7±0.4 mm for $Cx37^{+/+}$ littermates). In contrast, valve spacing was comparable between $Cx43^{+/-}$ and $Cx43^{+/+}$ vessels (1.3±0.4 mm and 1.4±0.2 mm, respectively). Cx40 immunostaining was not detected in popliteal LECs or LMCs, nor were we able to detect Cx47 in popliteal LECs or LMCs, although expression of Cx47 specifically in popliteal valve leaflets was not tested (Online Figure I). Previous work has shown that Cx47 immunostaining can be detected in some of

the LECs present in developing mesenteric lymphatic vessels (E18.5-P3), in mesenteric lymphatics from 4-week old mice, and in a restricted subset of valve LECs in adult thoracic duct [6]. A recent study using indirect methods for detecting Cx47 expression has reported more widespread Cx47 expression in LECs of adult lymphatic vessels [62].

New methods were needed to quantitatively assess how contraction waves are coordinated over the length of the lymphangion to evoke effective, propulsive contractions. Isolation, cannulation, and pressurization of these vessels *ex vivo* allowed stable pressure control critical for repeatable assessment of contractile activity. First, we assessed contractile function based on established methods for edge detection of internal diameter [63, 64], from which we can accurately assess tone, contraction frequency, and contraction amplitude at a single representative location along the vessel. We then developed techniques, adapted from methods previously utilized for GI studies[65–67], to measure the conduction speed and degree of synchronization of contraction waves. External vessel diameters were measured over time from high-speed (100–250 fps), brightfield videos of contractions at every position along the vessel length and the contraction pattern of the entire vessel was transformed into a two-dimensional Space Time Map (STM; see *Methods (Online Data Supplement)* section for detailed description). Figure 1A shows an STM representing 3 contractions of a WT (*C57BL/6*) vessel (see also Online Figure II and Online Video I). Further image processing and analysis of the STM (Figure 1A) allowed us to determine: 1) the initiation site of each contraction wave, 2) the direction of the contraction wave, 3) the conduction speed, and 4) the distance traveled along the lymphatic wall (expressed as percent of vessel length). Contractions for every vessel from WT mice consistently initiated at a single pacemaking site and, once initiated, every contraction propagated rapidly along the entire length of the cannulated segment at a consistent speed (Figure 1A). Entrained contractions were evident by nearly-straight, uniformly-spaced dark vertical bands extending from top to bottom (or vice versa) along the entire STM (Figure 1A). The uniform spacing of the bands indicated a consistent, stable contraction frequency. Transformation of the STMs into the frequency domain (Space Frequency Maps – SFMs) allowed analysis of the dominant frequencies (Figure 1B). Vessels from control mice consistently exhibited only a single dominant frequency.

We then used these new methods to characterize the contractile function of lymphatic vessels from mice deficient in specific Cx isoforms. Surprisingly, global deletions of Cx37 (*Cx37*$^{-/-}$ mice) or Cx47 (*Cx47*$^{-/-}$ mice) were not associated with an obvious abnormal contractile phenotype (Figure 1C,D). Likewise, vessels from *Lyve1-Cre;Cx43*$^{fx/fx}$ mice with lymphatic-specific endothelial deletion of Cx43 (global Cx43 deletion results in embryonic death) did not exhibit an abnormal contractile phenotype (Figure 1E). To comprehensively assess vessel function, we measured traditional contractile parameters based on internal diameter tracking at a representative site as well as parameters based on the STM and SFM to characterize contraction coordination/synchrony (conduction speed, number of initiation sites, spatial distribution of contraction frequencies, percent conduction length). None of these parameters were significantly different for vessels from *Cx37*$^{-/-}$, *Cx47*$^{-/-}$, or *Lyve1-Cre;Cx43*$^{fx/fx}$ mice compared to vessels from control (WT, *Cx43*$^{fx/fx}$) mice at a pressure of 3 cmH_2O (Figure 1F-I). Thus, contractions consistently initiated at a single pacemaking site and, once initiated, every contraction propagated rapidly along the entire length of the

cannulated segment at a consistent speed. Each vessel had a specific pressure-dependent frequency that was uniform throughout its entire length, as indicated by the narrow, white vertical-band on the SFM shown in Figure 1B. Mean conduction speed was 11.2±0.5 mm/s, and overall mean frequency was equal to 11.0±0.5 contractions per minute at an intraluminal pressure of 3 cmH_2O. Robust contractions, with a mean ejection fraction of 0.71±0.02 (at 3 cmH_2O), were consistently observed in all lymphatic segments from these Cx-deficient strains. Mean tone (expressed as percent of maximum passive diameter) and normalized contraction amplitude were not significantly different across all groups, with overall averages of 9.9±0.6% and 43.3±1.8% respectively. Conduction speed, number of initiation sites, percent conduction length, and ejection fraction measurements obtained at 3 cmH_2O intraluminal pressure for all groups are shown in Figure 1F-I. These analyses were sufficiently sensitive to detect subtle as well as overt defects on contraction synchrony, as will be evident in subsequent figures. Numerical comparisons of all contractile parameters (at 3 cmH_2O of pressure) for all groups are summarized in Online Table I.

The pressure dependency of contractile function was also assessed by calculating traditional contractile parameters (contraction amplitude, ejection fraction, frequency, and end diastolic diameter) for popliteal lymphatic vessels from Cx37, Cx43, or Cx47 deficient mice and their corresponding WT controls at seven different intraluminal pressures from 0.5 to 10 cmH_2O, spanning the presumed physiological range in the mouse [68, 69]. No significant differences in any of the contractile parameters were found between the groups at any pressure (Online Figure III). Previously, we showed that ACh inhibits contractions of mouse popliteal lymphatics purely through NO (nitric oxide) production[63]. Here we tested whether deletion of the known LEC Cx isoforms, Cx37, Cx43, or Cx47, would impair the response of popliteal lymphatics to ACh. When exposed to various ACh concentrations ranging from 1 to 100 nM, the contractile function and associated inhibition in vessels from the LEC Cx-deficient mice were not different from those of control vessels (Online Figure IV). Rather, normal responses to ACh that were blocked by L-NAME (10^{-4} M) were observed. Collectively, these results indicate that Cxs in the LEC layer are dispensable for the entrainment and conduction of lymphatic contraction waves and for NO-mediated inhibition of those contraction waves.

L-type Ca^{2+} channels, electrical coupling between LMCs and the apparent electrical isolation of the LMC layer are essential for the efficient propagation of action potentials.

Ca^{2+} influx through voltage-gated L-type Ca^{2+} channels is required for the initiation of lymphatic spontaneous contractions [70, 71], as it is for arterial constriction [72, 73]. In arterioles, an increase in intracellular Ca^{2+} in the smooth muscle layer can be accompanied by a subsequent elevation of intracellular Ca^{2+} in the endothelial cell layer [74, 75], due to the presence of myoendothelial gap junctions (MEGJs) that interconnect the two layers. Therefore, we hypothesized that measurement of Ca^{2+} signals in the smooth muscle and endothelial cell layers of popliteal lymphatics would allow us to assess if Ca^{2+} events in LMCs and possibly in LECs preceded spontaneous contractions, and if Ca^{2+} events in one layer spread to the other layer, possibly through MEGJs. To do this selectively in each layer, we generated two lines of mice expressing the fast Ca^{2+} indicator *GCaMP6f* in LMCs or LECs using SM- (smooth muscle-) or LEC-specific Cre-lines (*Smmhc-CreER^{T2};GCaMP6f*

or *Prox1-CreER^{T2};GCaMP6f*, respectively). Two weeks after induction with tamoxifen either the smooth muscle or endothelial cell layer of a pressurized popliteal lymphatic vessel was imaged on a confocal fluorescence microscope. High resolution videos of LMCs revealed two main classes of Ca^{2+} events. The first type were large-amplitude events that were highly-coordinated among all LMCs. Each spontaneous lymphatic contraction was preceded by one of these events, which we designated as *Ca^{2+} flashes* (Figure 2A and Online Videos II-III). Ca^{2+} flashes preceding each contraction conducted at the same rate as contraction waves (12.5±3.1 mm/s versus 12.2±2.0 mm/s, n=6, Figure 2A). Inhibition of L-type Ca^{2+} channels with nicardipine (300 nM) abolished both Ca^{2+} flashes and contractions (Figure 2B). These characteristic speeds are consistent, not with a conducted Ca^{2+} wave (which are known to travel at speeds of tens of microns per second), but with a wave of electrical depolarization that triggered global Ca^{2+} entry through L-type Ca^{2+} channels in every LMC. The second class of Ca^{2+} events consisted of low-amplitude, discrete events that occurred in almost every LMC, but which were not coordinated or synchronized between cells. These included Ca^{2+} events that resembled what previously have been designated in other tissues as *Ca^{2+} puffs* and *Ca^{2+} sparks*, based on their kinetics. Intracellular *Ca^{2+} waves* were also present in many LMCs, propagating at speeds from 30 – 200 μm/s within a LMC but not between LMCs (Figure 2C and Online Video IV).

Recordings of membrane potential in the LMC layer using a sharp microelectrode and imaging of the Ca^{2+} events in LMCs or LECs showed that rhythmic action potentials triggered Ca^{2+} flashes in the LMC layer. Action potentials originated from a baseline of -35.0±2.1 mV and peaked at -6.6±1.0 mV, with a duration of approximately 2 seconds). In contrast, the membrane potentials of endothelial cells were much more hyperpolarized (−69.5±1.3 mV) and remained extremely stable even as the overlaying muscle layer was firing action potentials (Figure 3A-D). Only rare, localized, non-coordinated Ca^{2+} events were observed in LECs (Figure 3E,F) despite an active LMC layer. LECs were uniformly silent unless stimulated with an agonist. The addition of 10 nM acetylcholine (ACh) to the bath triggered high frequency intracellular Ca^{2+} events in almost every LEC (Figure 3E,G and Online Video V).

Gap junction-mediated electrical communication between LMCs is required for the generation and entrainment of spontaneous contractions.

In mouse popliteal lymphatic vessels from WT mice, inhibition of gap junctional communication with 18β-glycyrrhetinic acid (18β-GA, 10–30 μM, n=4) disrupted the entrainment and propagation of spontaneous contractions, as evident by irregularly-spaced, wavy bands in the STM (Online Figure V). In contrast to control vessels, where uniform, vertical bands in the STM and a single peak in the SFM were indicative of rhythmic, rapidly-conducting contractions initiating from a single site, 18β-GA produced weaker contractions with variable and significantly reduced conduction speeds (~2- to 10-fold lower), multiple initiation sites, and an increased number of contraction frequencies that were variable even within the length of the cannulated lymphatic segment (Online Figure V and Online Video VI). Ca^{2+} imaging of the smooth muscle layer of popliteal lymphatics from *Smmhc-CreER^{T2};GCaMP6f* mice showed that after incubation with 18β-GA, Ca^{2+} flashes, and by inference the electrical depolarization wave, failed to be entrained and

propagated (Online Figure V and Online Video VII). These results confirm that electrical coupling of cells in the lymphatic wall is required to generate entrained, rapidly propagating contractions. When combined with the observation that deletion of the Cx isoforms normally expressed in the LEC layer did not impair conduction of contraction waves, and with the observation that the LMC and LEC layers appear electrically uncoupled, we conclude that Cxs mediating intercellular coupling between LECs play no detectable role in initiating, or modulating the coordination or strength of the spontaneous contractions of lymphatic vessels. Thus, the depolarizing, pacemaker signals that drive coordinated spontaneous contractions are generated in, and conducted exclusively through, the muscle layer via connexins in LMCs. The question then arises: what Cx isoforms in the LMC layer mediate conduction?

Human mesenteric and mouse popliteal lymphatics express similar Cx isoforms.

Entrainment of electrical and/or Ca^{2+} events between LMCs would require the expression of gap junction proteins (Cxs) in LMCs. Because the Cx isoforms in LMCs are unknown, we first assessed and compared Cx expression in both mouse popliteal lymphatics and human mesenteric lymphatic vessels. Human vessels were obtained from freshly excised sections of the jejunal wall of patients undergoing *roux-en-y* gastric bypass. On a nine Cx panel, results from End-Point RT-PCR assays showed that both mouse (n=3) and human (n=3) lymphatics (whole vessels) expressed mRNA for Cx37, Cx40, Cx43, Cx45, and Cx47, as well as for Cx26 and Cx30.2 (equivalent to human Cx31.9). Although the results from End-Point RT-PCR are qualitative, Cx37, Cx43, and Cx45 appeared to be the dominant isoforms (Figure 4B,D) in both species. Mouse brain and human intestine, respectively, were used as positive expression controls for these assays (Figure 4A,C). In the mouse, immunofluorescence images of popliteal lymphatic vessel thin sections confirmed protein expression for Cx45, which was localized primarily in the muscle layer of these murine lymphatics (Figure 4E-J). Also see Online Figure VI for additional Cx45 immunofluorescence images and their negative controls in mouse popliteal lymphatics.

Human mesenteric lymphatics express Cx45 and exhibit strong, coordinated spontaneous contractions.

Immunofluorescence imaging of human mesenteric lymphatic vessels also revealed Cx45 expression that appeared to be restricted mostly to the muscle layer (Figure 5A-C and Online Figure VI). When cannulated and pressurized, human collecting lymphatics developed strong, coordinated, spontaneous contractions that consistently initiated at a single pacemaking site and conducted rapidly (16.3±0.8 mm/s) along the length of the segment (Figure 5D-F and Online Video VIII). Human mesenteric lymphatics exhibited comparable contractile function to those of mouse popliteal lymphatics, as evidenced by similar contraction frequencies and ejection fractions over a range of intraluminal pressures (Figure 5G,H). As with mouse popliteal lymphatics, the contraction frequency of human mesenteric lymphatics increased as intraluminal pressure rose, was minimum at 0.5 cmH_2O (4.8±0.98 contractions/minute) and reached a plateau at around 5 cmH_2O (13.1±1.2 contractions/minute) (Figure 5G); ejection fractions ranged from 0.88±0.03 to 0.62±0.06 for intraluminal pressures between 0.5 and 3 cmH_2O (Figure 5H). Contraction amplitude and fractional pump flow were maximal at 1 cmH_2O and 2 cmH_2O, respectively (Online Figure

VII). Once stable, maximum tone (≥20%) was observed at pressures from 0.5–2 cmH_2O and consistently decreased as intraluminal pressure increased, reaching a minimum (7.0±1.9%) at 10 cmH_2O (Online Figure VII). Thus, the contractile parameters for human mesenteric lymphatics were remarkably similar to those for mouse popliteal lymphatics.

Lymphatic smooth muscle-specific deletion of GJC1 (Cx45) induces disruption of coordinated spontaneous contractions.

Since 18β-GA and other gap junction blockers are not specific for any Cx isoforms [53–55, 76] and also are known to have off-target effects on ion channels [77–79], we turned to genetic approaches to disrupt Cx function. We first considered Cx45 since it showed robust expression in both human and murine lymphatic vessels (Figure 4B,D). Two transgenic mouse models were utilized to assess the role of Cx45. We selectively deleted Cx45 from Nestin+ cells (Nestin is transiently and primarily expressed in LMCs during development) or LMCs using constitutive (*Nestin-Cre*) or tamoxifen [TMX]-inducible (*Smmhc-CreER^{T2}*) Cre lines, respectively. Due to the design of the $Cx45^{fx/fx}$ mouse (a gift from Klaus Willecke, University of Bonn), both *Nestin-Cre;Cx45$^{fx/fx}$* and *Smmhc-CreER^{T2};Cx45$^{fx/fx}$* vessels expressed GFP in all cells from which Cx45 was excised [48]. GFP fluorescence was observed in ~95% and >98% of popliteal LMCs in the two respective mouse lines, as determined by co-localization with smooth muscle actin (SMA, detected with a specific antibody) (Online Figure VIII). These results confirm our immunostaining results for Cx45 (Figure 4E-J). Popliteal lymphatic vessels from both *Nestin-Cre;Cx45$^{fx/fx}$* and *Smmhc-CreER^{T2};Cx45$^{fx/fx}$* mice exhibited a dramatic loss of coordination of LMC contractions (Figure 6B,C, Online Figure IX, and Online Video IX) when compared to control vessels (Figure 6A). LMC contractions were assessed in popliteal lymphatics from three different control groups: WT (*C57BL/6*) and *Cx45$^{fx/fx}$* mice, and tamoxifen injected *Cx45$^{fx/fx}$* mice. Groups of mice that were injected with tamoxifen, including controls, are labeled [TMX]. In order to rule out any potential effect of the tamoxifen treatment on the contractility of lymphatics, lymphatic function in vessels from the *Cx45$^{fx/fx}$*[TMX] control group was assessed 6–11 days post-induction. This is the earliest time point at which vessels from tamoxifen-induced *Smmhc-CreER^{T2};Cx45$^{fx/fx}$* mice were tested. Loss of coordination was evident in Cx45-deficient vessels by the development of multiple initiation sites (red open circles) and contraction waves that propagated over only a fraction of the vessel length and in multiple directions (yellow arrows) with slower and variable conduction speeds. The net result was a highly non-uniform STM and a corresponding SFM with multiple frequency components, reflecting the relative independence of the multiple initiation sites. The most striking effect of Cx45 deletion from the LMC layer was a ~10- to 18-fold reduction in conduction speed (Figure 7A). The number of initiation sites for contractions in Cx45 deficient vessels was significantly increased from the single site normally observed in control vessels to ~2–3 sites/mm (Figure 7B). Contractions from Cx45-deficient vessels failed to propagate through the entire length of the lymphatic segment under study (Figure 7C). Numerical results for all contractile parameters for Cx45-deficient and control vessels are listed in Online Table I. The mean length for lymphatic segments included in these studies, each containing 1–2 valves, was 1.19±0.06 mm.

To assess the consequences of SM-specific Cx45 deletion on Ca^{2+} signaling, we generated *Nestin-Cre;Cx45$^{fx/fx}$;GCaMP6f* mice expressing *GCaMP6f* in the LMC layer. After excision of Cx45, intracellular Ca^{2+} events were largely unchanged but the conduction speeds of propagated Ca^{2+} flashes were substantially reduced in *Nestin-Cre;Cx45$^{fx/fx}$;GCaMP6f* vessels compared to *Nestin-Cre;GCaMP6f* and *Smmhc-CreER^{T2};GCaMP6f* control vessels, and were comparable to those of the contraction waves propagating in the same vessels (Online Figure X). The lower conduction speeds and non-uniform, non-continuous band patterns of Ca^{2+} flashes in Cx45 deficient vessels, compared to fully entrained, uniform patterns of control vessels (Online Figure X) reinforce the results of the previous contraction wave analyses (Figures 6 and 7).

The dyssynchronous contraction waves and disrupted Ca^{2+} flashes observed in lymphatic vessels with SM-specific Cx45 deletion were not associated with any significant changes in LMC morphology. In a set of vessels from control (WT) and *Smmhc-CreER^{T2};Cx45$^{fx/fx}$* mice, we calculated the mean percent surface area of each lymphatic vessel that was covered by LMCs and LMC coverage was not significantly different between control and Cx-45 deficient vessels (Online Figure XI; 80.1±2.3% in control vessels (n=5) versus 78.1±2.6% in *Smmhc-CreER^{T2};Cx45$^{fx/fx}$* (n=6) vessels). As contractile efficiency would be maximal when all LMCs are oriented perpendicular to the longitudinal axis of the vessel, we measured the angle of cells at both non-valve and valve regions of control (N_{cells} = 754) and *Smmhc-CreER^{T2};Cx45$^{fx/fx}$* (N_{cells} = 860) vessels (n=6 vessels for each group). Here zero degrees represents a circumferential LMC. While the mean angles were significantly different between valve and non-valve regions, there were no significant differences between Cx45-deficient vessels compared to those from control mice in the two respective regions (Online Figure XI).

LMC-Cx45 deficient vessels exhibit impaired lymphatic pumping capability that worsens when challenged with an adverse pressure gradient.

In addition to a loss of entrainment of LMC contractions, significantly lower conduction speeds, and reduced conduction lengths in Cx45 deficient lymphatic vessels, spontaneous contractions in these vessels had significantly impaired ejection fractions (0.33±0.04 (n=9) for *Nestin-Cre;Cx45$^{fx/fx}$* and 0.17±0.02 (n=8) for *Smmhc-CreER^{T2};Cx45$^{fx/fx}$*) compared to the various control vessels, all of which exhibited ejection fractions >0.75 at 3 cmH_2O of intraluminal pressure (Figure 7D). These values were calculated based on the contraction amplitude measured at a single, representative site along the segment and factored in the corresponding mean percent conduction length. While local contraction amplitudes were not significantly different in vessels from Cx45-deficient mice compared to WT controls, the significantly shorter conduction lengths resulted in significantly impaired ejection fractions. Likewise, contraction frequency and tone were both significantly increased in Cx45 deficient vessels compared to their corresponding control groups (Figure 7E,F).

Because vessels from *Smmhc-CreER^{T2};Cx45$^{fx/fx}$* exhibited the most striking loss of contraction wave entrainment and speed 6–11 days post tamoxifen induction, we tested the ability of those vessels to pump/transport fluid against an adverse pressure gradient. Such tests required the use of 2-valve lymphatic segments (i.e. one complete lymphangion) with

independent input and output pressure control (Figure 8A). A servo-null micropipette (<3 μm tip diameter) was inserted through the vessel wall between the input and output valves to measure pressure in the central lymphangion [25]. Diameter was measured upstream from the output valve. Output valve position (open-closed) was monitored from continuous video recordings of contractions. In control vessels, each spontaneous contraction generated a propulsive pressure spike that subsequently opened the downstream valve (Figure 8C and Online Video X). The pressure spikes and the position of the output valve were monitored while output pressure was continuously increased, in ramp-wise fashion, from 1 to 12 cmH_2O until a pressure limit (P_{limit}) was reached when the output valve failed to open during lymphatic systole. Input pressure was maintained at 1 cmH_2O. While the fully coordinated lymphatic contractions in control vessels (*Cx45*$^{fx/fx}$[TMX]) were able to generate propulsive pressure spikes that opened the downstream valve up to an average adverse pressure of 9.4±0.5 cmH_2O (n=4), Cx45-deficient vessels (*Smmhc-CreER*^{T2}*;Cx45*$^{fx/fx}$[TMX], 6–11 days post induction) could only generate sufficiently strong pressure spikes to open the downstream valve at an average maximum adverse pressure of 4.6±0.6 cmH_2O (n=5) (Figure 8B). This index actually underestimated the degree of pump dysfunction because <50% of the contractions opened the output valve in Cx45 deficient vessels (Figure 8D) compared to 100% in control vessels (Figure 8C).

The loss of Cx45 may induce compensatory upregulation of other LMC Cxs.

Interestingly, 2–4 weeks after tamoxifen induction treatment was complete, lymphatic vessels from *Smmhc-CreER*^{T2}*;Cx45*$^{fx/fx}$ mice (n=6) exhibited a partial recovery of the coordination of LMC contractions compared to vessels 6–11 days post-induction, as evident by a reduction in the number of different initiation sites for contractions (from 3.1±0.3 sites/mm to 2.1±0.3 sites/mm), a slight but noticeable improvement in conduction speed (from 0.6±0.1 mm/s to 0.7±0.1 mm/s), and an enhanced conduction length (from 27.1±3.0% to 51.5±9.8%) (Figure 7A-C). Nine weeks post induction (n=4), the recovery in entrainment of LMC contractions was significantly improved from the 6–11-day group, when the number of initiation sites fell to 1.4±0.5 sites/mm, conduction speed increased to 1.9±0.1 mm/s, and contractions propagated through 74.8±12.6% of the vessel segment (Figure 7A-C). The partial recovery of entrainment of LMC contractions and increased conduction length were indicative of more LMCs being recruited by each pacemaking signal and resulted in more efficient contractions, as evident by a significant increase in ejection fraction from 0.17±0.02 at 6–11 days post induction to 0.37±0.07 at 2–4 weeks and 0.52±0.07 at 9 weeks post induction (Figure 7D). Normal contraction frequency and tone were also recovered ≥2–4 weeks following deletion of Cx45 (Figure 7E,F). Notably, the less severe loss of coordination in vessels from *Nestin-Cre;Cx45*$^{fx/fx}$ mice was maintained over time without a noticeable improvement. These results suggest a compensatory mechanism that is activated as a consequence of the sudden loss of Cx45 in mature, healthy lymphatics, perhaps involving the upregulation of other Cx isoforms that, under normal conditions, are not expressed in LMCs or are expressed at very low levels.

Disruption in contraction wave entrainment in popliteal lymphatic vessels from Cx45-deficient mice in vivo.

We then assessed the contractile function of lymphatic vessels from control and SM-specific Cx45-deficient mice in vivo. Following a 1–2 μL injection of FITC (2% w/v in sterile saline) at the dorsal aspect of the foot, fluorescence videos were collected of the actively contracting popliteal afferent lymphatic vessels. A contraction caused a rapid, transient drop in the fluorescence at each position along the vessel length. These changes in fluorescence were measured over time (using line-scan analysis) and represented as STMs with the fluorescence intensity encoded in grayscale. In vivo imaging of the contractile activity of popliteal lymphatic vessels from WT, *Smmhc-CreER^{T2};Cx45$^{fx/fx}$*, and *Nestin-Cre;Cx45$^{fx/fx}$* mice confirmed our *ex vivo* observations showing that SMC-deletion of Cx45 results in uncoordinated, slowly propagating contraction waves. In comparison to the uniform almost straight band patterns shown in the STM in Figure 9A, indicative of highly coordinated, fast propagating contractions, analyses of the in vivo contractions of Cx45-deficient vessels (Figure 9B,C) revealed STMs with disrupted, wavy band patterns. In agreement with our *ex vivo* studies, in vivo contractions of popliteal lymphatics from control mice were driven primarily by a single pacemaker and propagated through the entire field of view (2–3 mm); however, in some cases a second set of overlapping contractions (within the same field of view) were initiated at a different location by a second pacemaker, which resulted in colliding contraction waves and gave the impression of partially uncoordinated contractions. These multiple-pacemaker driven contractions appeared to be observed primarily at locations of lymphatic branches. In vivo, the conduction speed of spontaneous contractions of control vessels was 6.6±0.8 mm/s, compared to 1.1±0.2 mm/s for *Nestin-Cre;Cx45$^{fx/fx}$* and 1.4±0.2 mm/s for *Smmhc-CreER^{T2};Cx45$^{fx/fx}$* (Figure 9D). Consistent with the *ex vivo* results, the number of initiation sites was significantly increased and the conduction length significantly decreased in vessels from Cx-45 deficient compared to controls (Figure 9E-G).

Cx45 deficiency inhibits lymph transport only when mice are challenged with a gravitational load.

Finally, we assessed whether the impaired lymphatic pumping associated with SMC-specific deletion of Cx45 would impact transport in vivo. Following an injection (1–2 μL) of infrared dye (IRDye® 800CW PEG Contrast Agent) in the dorsal aspect of the foot, fluorescence videos were collected of the dye uptake and transport along the popliteal afferent lymphatic vessels using NIRF microscopy (Figure 10A and Online Figure XII). After injection, 0.5–3 minutes were generally required before dye uptake was initiated and began to appear in the collecting lymphatics. The wavefront of the fluorescent dye then moved downstream, advancing in a pulsatile manner with every contraction of the lymphatic vessel (Figure 10B). The wavefront was tracked from playback of the captured video images (at 1 fps) and mean transport speed was calculated. Lymph transport was thus assessed in the hindlimbs of control (*Cx45$^{fx/fx}$*) and Cx45-deficient (*Nestin-Cre;Cx45$^{fx/fx}$*) mice in horizontal (prone) and near-vertical positions. For the latter, the entire NIRF microscope was tilted to a ~78^{o} angle, imposing an acute gravitational load on the hindlimb. In the horizontal position, Cx45-deficiency resulted in a slight, but not significant, decrease in lymph transport speed (243.9±37.2 μm/s) compared to that of the control mice (335.5±34.9 μm/s). Under an imposed gravitational load in the near-vertical position, lymph transport was slightly, but not

significantly, reduced in control mice (225.7±29.9 μm/s), but was completely inhibited (for the duration of the ~8-minute observation period) in Cx45-deficient mice (Figure 10C). A related index of lymph transport, the distance traveled per minute, exhibited the same pattern: a slight but non-significant reduction in control mice when a gravitational load was imposed, but a profound reduction in Cx45-deficient mice under the same conditions (Figure 10D).

DISCUSSION

Genetic mutations most commonly linked to lymphedema in humans include *VEGFR3* [80–82], *CCBE1* [83–86], and *SOX18* [87, 88]. These mutations affect development, growth and proliferation of lymphatic vessels. Inherited (primary) lymphedema can also result from abnormal venous and lymphatic valve architecture [89–91] such as occurs in lymphedema distichiasis and CM-AVM (capillary malformation/arteriovenous malformation), caused by *FOXC2* [92–95] and *RASA1* [91, 96] deficiencies, respectively. In addition, three recent studies have described cases of primary lymphedema tied to mutations in Cxs. Ferrell et al. found dominantly inherited lymphedema in a group of families that resulted from six uniquely identified missense mutations in *GJC2* [1] (encoding Cx47), a Cx isoform that in the mouse is expressed preferentially in lymphatic and venous valves [6, 62, 97]. In adult veins, Cx47 appears to be restricted to a subset of venous endothelial cells on the upstream face of the venous valve leaflet [98]. Ostergaard et al. confirmed that autosomal dominant *GJC2* mutations in the extracellular domain of Cx47 were linked to lymphedema in four families [2]. Women with *GJC2* mutations were subsequently found to be more susceptible to developing secondary lymphedema after surgical intervention for breast cancer [3]. Recessive mutations in *GJC2* (Cx47) have been found to cause various disorders including Pelizaeus-Merzbacher-like disease (a severe dysmyelinating disorder) [99], hereditary spastic paraplegia [100], and subclinical leukodystrophy [101]. Interestingly, none of these mutants developed lymphedema, which suggests that dominant negative mutations in Cx47 may be required to cause primary lymphedema, perhaps through a negative impact on Cx43 expression and/or function. Various mutations in *GJA1* (Cx43) are known to cause oculodentodigital syndrome [102, 103], and at least one of those has been linked to primary lymphedema in three generations of a family [4]. The mechanisms underlying Cx-related lymphedema are unknown but could be related to the abnormal growth/development of lymphatic vessels, lymphatic valve defects, and/or lympho-venous valve defects. Indeed, a recent study demonstrated that patients with *FOXC2* or *GJC2* mutations show profound structural and functional defects in venous valves [37]. Alternatively, because Cxs mediate electrical communication between cells, Cx-related lymphedema could be caused by defects in signaling within or between the smooth muscle and endothelial layers of the lymphatic wall. Indeed, the authors of the studies cited above speculated that lymphedema in patients with Cx47 or Cx43 mutations may have resulted from *"impaired coordination of pulsatile lymphatic flow"*; however, this hypothesis has never been tested [1] and likely cannot be tested in humans with currently available methods.

Clues to the mechanism(s) by which Cx mutations cause primary lymphedema may be elucidated by transgenic mouse studies, where deficiencies in Cx37 and Cx43, two of the Cx isoforms expressed in mouse lymphatic endothelium, have been associated with various

vascular abnormalities in collecting lymphatic vessels. Severe lymphatic dysfunction is observed in *Cx37*$^{-/-}$;*Cx43*$^{+/-}$ double mutant mice, which exhibit a reduction in valve density, pronounced back-leak in intercostal and subdermal lymphatics, and eventually die of chylothorax [6]. The extent to which lymphatic valves are dysfunctional in mice singly deficient in Cx37 or Cx47 is not clear. Backflow tests using Evans Blue or fluorescence tracers in vivo are suggestive of dysfunction, but such tests are not definitive because valve competency is strongly dependent on diameter [25, 104], which is determined by pressure and vessel tone, and both variables are unknown in traditional tests of backflow in vivo. Although *ex vivo* valve tests were not the focus of the present study, we noted reduced numbers of lymphatic valves in *Cx37*$^{-/-}$ popliteal vessels and observed that a valve in one of two tested *Cx37*$^{-/-}$ vessels was abnormally leaky and failed to close in response to extreme elevation of output pressure. In addition, we recently reported that complete deletion of Cx43 from the lymphatic endothelium (using *Lyve1-Cre;Cx43*$^{fx/fx}$ mice) results in reduced lymphatic valve frequency and valves that exhibit reflux even when closed, leading to insufficient lymph transport and chylothorax [57]. Thus, it is likely that valve defects underlie or contribute to lymphedema in patients with Cx43 or Cx47 mutations. Defective venous valves can be detected in humans using Doppler ultrasound [37, 105], but such tests have not yet been applied to lymphatic valves, let alone to lymphatic valves in patients with Cx43 or Cx47 mutations.

The primary focus of our study was to test the hypothesis that deletion or deficiency of LEC-Cxs would impair the coordination of spontaneous, propulsive contractions in collecting lymphatic vessels. Electrical coupling between LMCs likely is required for efficient pumping by these vessels, as action potentials in the muscle layer drive spontaneous contractions and the resulting contractions account for two-thirds of peripheral lymph transport [106]. However, it is also possible that homocellular electrical coupling between LECs, and/or heterocellular coupling between LMCs and LECs, is/are critical for the coordination of lymphatic contraction waves. The precedent for this idea comes from the blood vessel literature where it is well established that tight electrical coupling of ECs through Cx40 [107–109], and possibly other Cx isoforms, is the major conduction pathway for hyperpolarization signals. These signals can originate even in downstream capillary networks [110–113], be conducted along the endothelium, and be transmitted to the smooth muscle layer through MEGJs, leading to the coordinated, rapid, and robust vasodilation of upstream arterioles and small arteries - a phenomenon known as ascending vasodilation [41, 42]. To test the possible role of conducted responses through the LEC layer, we developed new methods to quantitatively assess contraction wave entrainment and investigated the role of Cx-mediated cellular communication in the contractile function of popliteal afferent lymphatic vessels under controlled conditions *ex vivo*. We find that the entrainment of contraction waves in vessels from *Cx37*$^{-/-}$ or *Cx47*$^{-/-}$ mice does not differ significantly from that of control vessels. Likewise, the entrainment of contraction waves in Cx43-deficient vessels (vessels from *Cx43*$^{+/-}$, *Lyve1-Cre;Cx43*$^{fx/fx}$, *Lyve1-Cre;Cx43*$^{fx/+}$, or *Lyve1-Cre;Cx43*$^{fx/\Delta}$ mice) is not significantly different from that of their corresponding controls. Neither could we detect significant lymphatic contractile deficiencies (contraction amplitude, ejection fraction, calculated pump flow) after deletion of any of these three Cxs normally expressed in LECs. The latter result is consistent with a recent report showing a

lack of obvious contractile dysfunction in inguinal-axillary lymphatics from *Cx47*$^{-/-}$ mice in vivo [62]. Thus, although Cx37, Cx43, and Cx47 may be critical for the normal development and number of lymphatic valves in the mouse, our results suggest that these endothelial Cxs are dispensable for the generation, coordination, and conduction of the electrical signals that drive the spontaneous contractions of mature collecting lymphatic vessels. Extrapolation of these results to humans suggests that lymphedema in patients with Cx47 or Cx43 mutations is not caused by coordination or pumping defects but rather to reduced density and/or function of valves in the lymphatic vasculature. An alternative explanation is defects in the lymphovenous valves (LVVs), where lymph is returned to the bloodstream [29], as abnormal formation of LVVs has been reported in various transgenic mouse models used for the study of primary lymphedema [5]. Our findings do not exclude other important roles for Cx37, Cx43, and Cx47 in the function of LECs in mature mice, such as processes that might require cell-cell communication in the endothelial layer.

Although there is substantial information about Cx isoform expression in the lymphatic endothelium showing the critical involvement of some isoforms in the normal development of the lymphatic vasculature, less is known about the functional roles of lymphatic Cxs in mature vessels [114]. For example, whether lymphatic vessels have an internal elastic lamina with EC projections and MEGJs that allow direct heterocellular communication, i.e. electrical coupling and/or diffusion of small molecules between LECs and LMCs, remains unknown. A single study in guinea pig mesenteric lymphatics suggests that communication between the two layers may be limited [115]. Having ruled out a critical role for LEC Cxs in the coordination of lymphatic contraction waves, we examined the roles of Cxs in the LMC layer. No previous studies have determined which Cx isoforms are expressed in lymphatic muscle, although three studies have provided indirect evidence for electrical coupling through Cxs using non-specific gap junction inhibitors [53–55]. Here, we identify Cx45 as a major Cx isoform in the lymphatic smooth muscle layer. We demonstrated Cx45 expression in popliteal afferent lymphatics and in human mesenteric lymphatic vessels by both PCR and immunofluorescence imaging and confirmed its expression in mouse lymphatics by GFP expression after Cx45 excision in two transgenic mouse lines (*Nestin-Cre;Cx45*$^{fx/fx}$ and *Smmhc-CreER*^{T2}*;Cx45*$^{fx/fx}$). In control lymphatic vessels, the contractions of all LMCs within a lymphangion, and even across valves to adjacent lymphangions, typically are fully entrained and initiated from a single pacemaking site. In contrast, vessels from mice lacking Cx45 in the smooth muscle layer exhibit partial-to-severe loss of contraction coordination between LMCs. As a consequence, significantly more initiation sites for contractions are observed, resulting in a higher contraction frequency due to multiple active pacemakers. Once initiated, each contraction wave propagates over a significantly shorter distance from the pacemaking site, indicative of a significantly smaller number of LMCs that can be simultaneously recruited/entrained by a single pacemaking signal. The most dramatic effect of SM-specific Cx45 deletion is a ~10- to 18-fold reduction in conduction speed associated with the propagation of contractions, which implies an increase in cell-to-cell resistance to current flow. Another consequence of reduced electrical coupling between LMCs is that each pacemaking stimulus results in a more localized contraction, with a significantly impaired ejection fraction as determined for the whole vessel. After deletion of Cx45 in LMCs, the Ca^{2+} flashes observed in that layer are not only disrupted and fail to propagate as

far as those in control vessels, but also propagate with a significantly lower speed (≤ 1 mm/s), consistent with our brightfield measurements of contraction wave propagation. These observations predicted defective pump function in Cx45-deficient lymphatic vessels, which was confirmed by pump tests in which 2-valve lymphangions were unable to generate sufficient systolic pressure to transport fluid against an increasing adverse pressure gradient. Thus, the uncoordinated, short and slowly-conducting contraction waves in Cx45-deficient vessels result in contractions that cannot efficiently propel lymph against an adverse pressure gradient. In vivo assessment of the contractile activity of popliteal lymphatics from control and Cx45-deficient (SMC-deficiency) mice confirmed our observations of isolated vessels. Interestingly, conduction speed in lymphatics from control mice measured in vivo was lower than that measured in isolated segments, which is expected due to the larger current sinks created by the longer segment lengths and their coupling to lymphatic networks.

Lymphatic vessels from *Smmhc-CreER^{T2};Cx45$^{fx/fx}$* mice exhibit a more severe contractile phenotype when compared to those from *Nestin-Cre;Cx45$^{fx/fx}$* animals. While the less severe contraction deficiencies associated with the deletion of Cx45 using the (constitutive) *Nestin-Cre* line remain constant over time, some aspects of contractile dysfunction in (inducible) *Smmhc-Cre;Cx45$^{fx/fx}$* vessels exhibit a time-dependent recovery. Contractions in *Smmhc-CreER^{T2};Cx45$^{fx/fx}$* vessels are most severely affected at 6–11 days post induction with tamoxifen (we did not test earlier time-points 1–5 days post induction). However, contractions begin to recover over time and improvement was significant even after only 2 weeks post induction, with all contractile parameters except for conduction speed being partially restored by 9 weeks (time points between 4 and 9 weeks were not tested). These results, coupled with the observation that Cx45-deficient vessels do not show a complete loss of coordination (i.e. synchrony persists over short distances), point to a compensatory upregulation of one or more different LMC Cx isoforms in response to Cx45 deletion. The persistence of a significantly lower conduction speed (≤ 2 mm/s, ~5-fold slower than controls) in *Smmhc-CreER^{T2};Cx45$^{fx/fx}$* 9 weeks after induction suggests that Cx45 is being replaced with a Cx isoform that forms either homomeric or heteromeric gap junctions with slower gating dynamics. Additional studies in the mouse, perhaps involving the double-deletion of Cx45 and other Cx isoforms present in the smooth muscle layer, may be necessary to completely explain the apparent residual coupling between Cx45-deficient LMCs.

Our studies are the first to assess spontaneous contractions of pressurized human lymphatics. Based on our results, human and mouse lymphatics exhibit similar contractile properties and similar Cx isoform expression patterns, with both species expressing Cx45 in the muscle layer; these observations suggest that Cx45 may be critical for lymphatic contractions and efficient lymph transport in humans. Very little is known about *GJC1* (encoding Cx45) mutations [36, 116] and their potential pathogenic roles. Although electrical signals in the heart are normally mediated by the most prevalent gap junction, Cx43, Cx45 is critical in the conduction system [117, 118], especially during development, and its upregulation in the left ventricle results in ventricular arrhythmias due to abnormal propagation of electrical impulses and heart failure [119, 120]. A single study reported that a Cx45 mutation (p.R75H) is associated with congenital atrioventricular block and progressive defects in the atrial conduction system that ultimately result in atrial standstill [116]. In the mouse, global

deficiency of Cx45 results in embryonic death due to cardiac failure during the early stages of heart development [121]. These findings suggest that many/most Cx45 mutations in humans may be lethal and therefore not detected in clinical screens for primary lymphedema using whole exome sequencing.

Does loss of contraction wave entrainment lead to lymphedema? This question is difficult to answer in mice for several reasons. Lymphedema in adult mice has only been demonstrated in a few cases where lymphatic tracts/valves are severely disrupted or missing altogether. Examples include 1) the mouse tail model in which both superficial and deep (collecting) lymphatic vessels are disrupted surgically, resulting in measurable swelling of the tail circumference within a few days, but which subsequently resolves as newly-formed vessels bridge the damaged region[122–124]; 2) Chy mice, with altered VEGFR3 signaling, lack initial and collecting lymphatics in some regions (including the hindlimb) and exhibit elevated interstitial hydrostatic pressure and hindpaw swelling[125]. Human patients with lymphatic tract disruption due to surgery or VEGFR3 mutations also develop lymphedema[80–82, 126]. However, many other genetic defects of the lymphatic system that produce primary lymphedema in humans (almost always in the extremities) do *not* produce lymphedema in mice. Examples include FOXC2$^{+/-}$ patients, as well as patients with Cx43 or Cx47 mutations, as described above.

The explanation for the increased susceptibility of humans to lymphedema, and its high incidence in the limbs in particular, is undoubtedly related to the effect of gravity on the balance of forces controlling interstitial fluid volume. For this reason, we hypothesized that mouse lymphatic contractile defects would be exaggerated under a gravitational load. We estimated that placing the mouse in a near-vertical position (~78^{o} degrees) would impose a ~5 cmH_2O hydrostatic load on the lymphatics in the hindlimb. Based on our *ex vivo* results (Figure 8B,D), where Cx45-deficient vessels only inconsistently overcame a ~4 cmH_2O output pressure load (i.e. some propulsion every 3–4 contraction cycles), we would have expected some transport to continue under comparable conditions in vivo, but at a lower rate and with increased transit time; indeed, these predictions are in agreement with our in vivo results in Figure 10. Dye transport in popliteal lymphatics from healthy, control mice in a near-vertical position results in a ~33% (but not statistically significant) reduction in lymph transport compared to measurements obtained in a horizontal position, and where the imposed hydrostatic pressure (<1 cmH_2O) can be overcome by the pressure spike generated during each lymphatic contraction cycle. However, the differences in transport between the two body positions are exaggerated in mice with smooth muscle-specific Cx45-deficiency (Figure 10). These results show that even a modest gravitational load reflecting a natural body position can exacerbate a lymphatic defect. By extrapolation, this significant defect in lymph transport would lead to hindlimb lymphedema if the mice could be *chronically* subjected to a comparable gravitational load. Whether detectable lymphedema would require days, weeks, or even months to develop is unknown. The observation that FOXC2$^{+/-}$ patients do not develop lymphedema until around puberty[92, 127, 128] suggests that this process might require a substantial length of time. In mice it is not testable with current methodology nor would testing likely be permitted under current animal guidelines (i.e. restraining unanesthetized animals in a vertical position for prolonged periods of time). Direct measurement of subtle and/or acute changes in interstitial fluid volume in mice awaits

the development of more sensitive techniques because the current method (wet:dry tissue weight ratio) is relatively insensitive, traumatic (requiring skin patch removal), and cannot be used repetitively over time[129, 130].

Apart from their clinical significance, our results have important implications for lymphatic physiology. Our Ca^{2+} imaging and membrane potential recordings in LECs and LMCs show that highly-entrained Ca^{2+} flashes, driven by rhythmic and synchronized action potentials, occur in all LMCs while the endothelial layer remains quiescent. In addition, the resting membrane potentials of LMCs and LECs are strikingly different (−35 mV and −70 mV, respectively), in contrast to the blood vasculature where the membrane potentials of SMCs and ECs are similar and are synchronized via heterocellular coupling through MEGJs [131, 132]. This difference implies limited-to-non-existent electrical coupling between LECs and LMCs [115] and suggests that the lymphatic wall may be optimized for conducting depolarizing current and constriction in contrast to the arteriolar wall, which is optimized for conducting hyperpolarization and dilation [41]. Electrical isolation of the lymphatic muscle layer from other surrounding cell networks, including the endothelium, may not only be a unique characteristic of the lymphatic vasculature, but may be required for the focal generation of pacemaking signals and action potentials and the resulting entrained depolarization waves that drive the spontaneous contractions of lymphatic collectors. Our results also reveal important insights about the mechanisms underlying lymphatic pacemaking. Pacemaking signals normally appear to originate at the ends of isolated, cannulated lymphatic segments; however, in Cx45 deficient vessels, multiple initiation sites develop in the middle regions of the vessels irrespective of valve position, which suggests that any LMC can become a pacemaker. Future studies recording membrane potential and elementary Ca^{2+} events simultaneously from these cells may aid in identification of the ionic mechanisms underlying pacemaking. Investigation of the electrical and/or Ca^{2+} signaling at the pacemaking site itself is a present limitation not only for lymphatic physiology, but also for other tissues with spontaneous electrical activity, including the heart, the gastrointestinal tract, and the nervous system, where pacemaking signals almost always originate outside the field of view, limiting inquiry to mechanisms of propagation but not pacemaking initiation.

In conclusion, our results 1) identify Cx45 as the critical Cx mediating the entrainment of the electrical signals, Ca^{2+} flashes and subsequent contraction waves in lymphatic smooth muscle; 2) indicate that endothelial Cx isoforms are dispensable for the generation, coordination, and conduction of those contractions; 3) reveal an apparent uncoupling of electrical and Ca^{2+} signals between LECs and LMCs; 4) significantly expand what is known about cell-to-cell communication in the lymphatic wall; 5) allow us to understand the mechanism(s) through which Cx mutations and aberrant electrical coupling in the lymphatic muscle layer could result in impaired lymph transport potentially leading to lymphedema; 6) suggest that lymphedema in patients with Cx47 or Cx43 mutations is not caused by disrupted lymphatic contraction waves but rather by impaired lymph transport due to abnormal valve development and/or reduced valve density; and 7) suggest that many murine models of lymphatic dysfunction, including Cx45 deficiency, may not develop lymphedema unless a chronic gravitational load is imposed.

Supplementary Material

Refer to Web version on PubMed Central for supplementary material.

ACKNOWLEDGEMENTS

The authors are grateful for the expert technical assistance of Shanyu Ho. We acknowledge Steffan Offermanns, Klaus Willecke and Taija Mäkinen for permission to use mice generated in their laboratories and Gwen Randolph for generous provision of fixed human lymphatic vessels used for some staining protocols.

SOURCES OF FUNDING

This work was supported by NIH grants HL-125608, HL-122578, and HL120867 to MJD.

Nonstandard Abbreviations and Acronyms:

Cx	connexin
LMC	lymphatic muscle cell
LEC	lymphatic endothelial cell
SMC	smooth muscle cell
EC	endothelial cell
18β-GA	18β-glycyrrhetinic acid
STM	space time map
SFM	space frequency map
TMX	tamoxifen
MEGJ	myoendothelial gap junction
LVV	lymphovenous valve
Ach	acetylcholine
NO	nitric oxide
FITC	fluorescein isothiocyanate-dextran
NIRF	near infrared fluorescence

REFERENCES

1. Ferrell RE, Baty CJ, Kimak MA, Karlsson JM, Lawrence EC, Franke-Snyder M, Meriney SD, Feingold E, Finegold DN. Gjc2 missense mutations cause human lymphedema. Am J Hum Genet. 2010;86:943–948 [PubMed: 20537300]
2. Ostergaard P, Simpson MA, Brice G, Mansour S, Connell FC, Onoufriadis A, Child AH, Hwang J, Kalidas K, Mortimer PS, Trembath R, Jeffery S. Rapid identification of mutations in gjc2 in primary lymphoedema using whole exome sequencing combined with linkage analysis with delineation of the phenotype. J Med Genet. 2011;48:251–255 [PubMed: 21266381]

3. Finegold DN, Baty CJ, Knickelbein KZ, Perschke S, Noon SE, Campbell D, Karlsson JM, Huang D, Kimak MA, Lawrence EC, Feingold E, Meriney SD, Brufsky AM, Ferrell RE. Connexin 47 mutations increase risk for secondary lymphedema following breast cancer treatment. Clin Cancer Res. 2012;18:2382–2390 [PubMed: 22351697]
4. Brice G, Ostergaard P, Jeffery S, Gordon K, Mortimer PS, Mansour S. A novel mutation in gja1 causing oculodentodigital syndrome and primary lymphoedema in a three generation family. Clin Genet. 2013;84:378–381 [PubMed: 23550541]
5. Geng X, Cha B, Mahamud MR, Lim KC, Silasi-Mansat R, Uddin MK, Miura N, Xia L, Simon AM, Engel JD, Chen H, Lupu F, Srinivasan RS. Multiple mouse models of primary lymphedema exhibit distinct defects in lymphovenous valve development. Dev Biol. 2016;409:218–233 [PubMed: 26542011]
6. Kanady JD, Dellinger MT, Munger SJ, Witte MH, Simon AM. Connexin37 and connexin43 deficiencies in mice disrupt lymphatic valve development and result in lymphatic disorders including lymphedema and chylothorax. Dev Biol. 2011;354:253–266 [PubMed: 21515254]
7. Sabine A, Agalarov Y, Maby-El Hajjami H, Jaquet M, Hagerling R, Pollmann C, Bebber D, Pfenniger A, Miura N, Dormond O, Calmes JM, Adams RH, Makinen T, Kiefer F, Kwak BR, Petrova TV. Mechanotransduction, prox1, and foxc2 cooperate to control connexin37 and calcineurin during lymphatic-valve formation. Dev Cell. 2012;22:430–445 [PubMed: 22306086]
8. Modi S, Stanton AW, Svensson WE, Peters AM, Mortimer PS, Levick JR. Human lymphatic pumping measured in healthy and lymphoedematous arms by lymphatic congestion lymphoscintigraphy. J Physiol. 2007;583:271–285 [PubMed: 17569739]
9. Olszewski WL. Contractility patterns of normal and pathologically changed human lymphatics. Ann N Y Acad Sci. 2002;979:52–63; discussion 76–59 [PubMed: 12543716]
10. Olszewski WL, Engeset A. Intrinsic contractility of prenodal lymph vessels and lymph flow in human leg. Am J Physiol. 1980;239:H775–783 [PubMed: 7446752]
11. Stanton AW, Modi S, Bennett Britton TM, Purushotham AD, Peters AM, Levick JR, Mortimer PS. Lymphatic drainage in the muscle and subcutis of the arm after breast cancer treatment. Breast Cancer Res Treat. 2009;117:549–557 [PubMed: 19052859]
12. Mortimer PS, Levick JR. Chronic peripheral oedema: The critical role of the lymphatic system. Clin Med (Lond). 2004;4:448–453 [PubMed: 15536876]
13. Rockson SG, Rivera KK. Estimating the population burden of lymphedema. Ann N Y Acad Sci. 2008;1131:147–154 [PubMed: 18519968]
14. Witte CL, Witte MH. Disorders of lymph flow. Acad Radiol. 1995;2:324–334 [PubMed: 9419570]
15. Witte MH, Dumont AE, Clauss RH, Rader B, Levine N, Breed ES. Lymph circulation in congestive heart failure: Effect of external thoracic duct drainage. Circulation. 1969;39:723–733 [PubMed: 5785287]
16. Leduc O, Crasset V, Leleu C, Baptiste N, Koziel A, Delahaie C, Pastouret F, Wilputte F, Leduc A. Impact of manual lymphatic drainage on hemodynamic parameters in patients with heart failure and lower limb edema. Lymphology. 2011;44:13–20 [PubMed: 21667818]
17. Wegria R, Zekert H, Walter KE, Entrup RW, De Schryver C, Kennedy W, Paiewonsky D. Effect of systemic venous pressure on drainage of lymph from thoracic duct. Am J Physiol. 1963;204:284–288 [PubMed: 13999501]
18. Greene AK, Grant FD, Slavin SA. Lower-extremity lymphedema and elevated body-mass index. N Engl J Med. 2012;366:2136–2137
19. Weitman ES, Aschen SZ, Farias-Eisner G, Albano N, Cuzzone DA, Ghanta S, Zampell JC, Thorek D, Mehrara BJ. Obesity impairs lymphatic fluid transport and dendritic cell migration to lymph nodes. PLoS One. 2013;8:e70703 [PubMed: 23950984]
20. Rockson SG. Precipitating factors in lymphedema: Myths and realities. Cancer. 1998;83:2814–2816 [PubMed: 9874403]
21. Clough G, Smaje LH. Simultaneous measurement of pressure in the interstitium and the terminal lymphatics of the cat mesentery. J Physiol. 1978;283:457–468 [PubMed: 722586]
22. Hargens AR, Zweifach BW. Contractile stimuli in collecting lymph vessels. Am J Physiol. 1977;233:H57–65 [PubMed: 879337]

23. Drake RE, Gabel JC. Effect of outflow pressure on intestinal lymph flow in unanesthetized sheep. Am J Physiol. 1991;260:R668–671 [PubMed: 2012238]
24. Hargens AR, Millard RW, Pettersson K, Johansen K. Gravitational haemodynamics and oedema prevention in the giraffe. Nature. 1987;329:59–60 [PubMed: 3627240]
25. Davis MJ, Rahbar E, Gashev AA, Zawieja DC, Moore JE, Jr. Determinants of valve gating in collecting lymphatic vessels from rat mesentery. Am J Physiol Heart Circ Physiol. 2011;301:H48–60 [PubMed: 21460194]
26. Eisenhoffer J, Kagal A, Klein T, Johnston MG. Importance of valves and lymphangion contractions in determining pressure gradients in isolated lymphatics exposed to elevations in outflow pressure. Microvasc Res. 1995;49:97–110 [PubMed: 7746166]
27. Schmid-Schonbein GW. Microlymphatics and lymph flow. Physiol Rev. 1990;70:987–1028 [PubMed: 2217560]
28. von der Weid PY, Zawieja DC. Lymphatic smooth muscle: The motor unit of lymph drainage. Int J Biochem Cell Biol. 2004;36:1147–1153 [PubMed: 15109561]
29. Srinivasan RS, Oliver G. Prox1 dosage controls the number of lymphatic endothelial cell progenitors and the formation of the lymphovenous valves. Genes Dev. 2011;25:2187–2197 [PubMed: 22012621]
30. Zhang R, Taucer AI, Gashev AA, Muthuchamy M, Zawieja DC, Davis MJ. Maximum shortening velocity of lymphatic muscle approaches that of striated muscle. Am J Physiol Heart Circ Physiol. 2013;305:H1494–1507 [PubMed: 23997104]
31. Pfenniger A, Wohlwend A, Kwak BR. Mutations in connexin genes and disease. Eur J Clin Invest. 2011;41:103–116 [PubMed: 20840374]
32. Dobrowolski R, Willecke K. Connexin-caused genetic diseases and corresponding mouse models. Antioxid Redox Signal. 2009;11:283–295 [PubMed: 18831677]
33. Goodenough DA, Paul DL. Beyond the gap: Functions of unpaired connexon channels. Nat Rev Mol Cell Biol. 2003;4:285–294 [PubMed: 12671651]
34. Bosco D, Haefliger JA, Meda P. Connexins: Key mediators of endocrine function. Physiol Rev. 2011;91:1393–1445 [PubMed: 22013215]
35. Meens MJ, Sabine A, Petrova TV, Kwak BR. Connexins in lymphatic vessel physiology and disease. FEBS Lett. 2014;588:1271–1277 [PubMed: 24457200]
36. Srinivas M, Verselis VK, White TW. Human diseases associated with connexin mutations. Biochim Biophys Acta. 2017
37. Lyons O, Saha P, Seet C, Kuchta A, Arnold A, Grover S, Rashbrook V, Sabine A, Vizcay-Barrena G, Patel A, Ludwinski F, Padayachee S, Kume T, Kwak BR, Brice G, Mansour S, Ostergaard P, Mortimer P, Jeffery S, Brown N, Makinen T, Petrova TV, Modarai B, Smith A. Human venous valve disease caused by mutations in foxc2 and gjc2. J Exp Med. 2017
38. Little TL, Beyer EC, Duling BR. Connexin 43 and connexin 40 gap junctional proteins are present in arteriolar smooth muscle and endothelium in vivo. Am J Physiol. 1995;268:H729–739 [PubMed: 7864199]
39. Looft-Wilson RC, Payne GW, Segal SS. Connexin expression and conducted vasodilation along arteriolar endothelium in mouse skeletal muscle. J Appl Physiol (1985). 2004;97:1152–1158 [PubMed: 15169746]
40. Simon AM, McWhorter AR. Vascular abnormalities in mice lacking the endothelial gap junction proteins connexin37 and connexin40. Dev Biol. 2002;251:206–220 [PubMed: 12435353]
41. Segal SS. Cell-to-cell communication coordinates blood flow control. Hypertension. 1994;23:1113–1120 [PubMed: 8206602]
42. Segal SS, Duling BR. Communication between feed arteries and microvessels in hamster striated muscle: Segmental vascular responses are functionally coordinated. Circ Res. 1986;59:283–290 [PubMed: 3769148]
43. Hald BO, Jacobsen JC, Sandow SL, Holstein-Rathlou NH, Welsh DG. Less is more: Minimal expression of myoendothelial gap junctions optimizes cell-cell communication in virtual arterioles. J Physiol. 2014;592:3243–3255 [PubMed: 24907303]
44. Hald BO, Welsh DG, Holstein-Rathlou NH, Jacobsen JC. Origins of variation in conducted vasomotor responses. Pflugers Arch. 2015;467:2055–2067 [PubMed: 25420525]

45. Welsh DG, Tran CHT, Hald BO, Sancho M. The conducted vasomotor response: Function, biophysical basis, and pharmacological control. Annu Rev Pharmacol Toxicol. 2017
46. Lampe PD, TenBroek EM, Burt JM, Kurata WE, Johnson RG, Lau AF. Phosphorylation of connexin43 on serine368 by protein kinase c regulates gap junctional communication. J Cell Biol. 2000;149:1503–1512 [PubMed: 10871288]
47. Jacobsen NL, Pontifex TK, Li H, Solan JL, Lampe PD, Sorgen PL, Burt JM. Regulation of cx37 channel and growth-suppressive properties by phosphorylation. J Cell Sci. 2017;130:3308–3321 [PubMed: 28818996]
48. Schmidt VJ, Jobs A, von Maltzahn J, Worsdorfer P, Willecke K, de Wit C. Connexin45 is expressed in vascular smooth muscle but its function remains elusive. PLoS One. 2012;7:e42287 [PubMed: 22848755]
49. Wang LJ, Liu WD, Zhang L, Ma KT, Zhao L, Shi WY, Zhang WW, Wang YZ, Li L, Si JQ. Enhanced expression of cx43 and gap junction communication in vascular smooth muscle cells of spontaneously hypertensive rats. Mol Med Rep. 2016;14:4083–4090 [PubMed: 27748857]
50. Wang LJ, Ma KT, Shi WY, Wang YZ, Zhao L, Chen XY, Li XZ, Jiang XW, Zhang ZS, Li L, Si JQ. Enhanced gap junctional channel activity between vascular smooth muscle cells in cerebral artery of spontaneously hypertensive rats. Clin Exp Hypertens. 2017;39:295–305 [PubMed: 28513236]
51. Fang JS, Angelov SN, Simon AM, Burt JM. Cx37 deletion enhances vascular growth and facilitates ischemic limb recovery. Am J Physiol Heart Circ Physiol. 2011;301:H1872–1881 [PubMed: 21856908]
52. Fang JS, Angelov SN, Simon AM, Burt JM. Cx40 is required for, and cx37 limits, postischemic hindlimb perfusion, survival and recovery. J Vasc Res. 2012;49:2–12 [PubMed: 21986401]
53. Crowe MJ, von der Weid PY, Brock JA, Van Helden DF. Co-ordination of contractile activity in guinea-pig mesenteric lymphatics. J Physiol. 1997;500 (Pt 1):235–244 [PubMed: 9097947]
54. McHale NG, Meharg MK. Co-ordination of pumping in isolated bovine lymphatic vessels. J Physiol. 1992;450:503–512 [PubMed: 1432715]
55. Zawieja DC, Davis KL, Schuster R, Hinds WM, Granger HJ. Distribution, propagation, and coordination of contractile activity in lymphatics. Am J Physiol. 1993;264:H1283–1291 [PubMed: 8476104]
56. Kanady JD, Munger SJ, Witte MH, Simon AM. Combining foxc2 and connexin37 deletions in mice leads to severe defects in lymphatic vascular growth and remodeling. Dev Biol. 2015;405:33–46 [PubMed: 26079578]
57. Munger SJ, Davis MJ, Simon AM. Defective lymphatic valve development and chylothorax in mice with a lymphatic-specific deletion of connexin43. Dev Biol. 2017;421:204–218 [PubMed: 27899284]
58. Pfenniger A, Meens MJ, Pedrigi RM, Foglia B, Sutter E, Pelli G, Rochemont V, Petrova TV, Krams R, Kwak BR. Shear stress-induced atherosclerotic plaque composition in apoe(−/−) mice is modulated by connexin37. Atherosclerosis. 2015;243:1–10 [PubMed: 26342936]
59. Schulte-Merker S, Sabine A, Petrova TV. Lymphatic vascular morphogenesis in development, physiology, and disease. J Cell Biol. 2011;193:607–618 [PubMed: 21576390]
60. Sabine A, Bovay E, Demir CS, Kimura W, Jaquet M, Agalarov Y, Zangger N, Scallan JP, Graber W, Gulpinar E, Kwak BR, Makinen T, Martinez-Corral I, Ortega S, Delorenzi M, Kiefer F, Davis MJ, Djonov V, Miura N, Petrova TV. Foxc2 and fluid shear stress stabilize postnatal lymphatic vasculature. J Clin Invest. 2015;125:3861–3877 [PubMed: 26389677]
61. Zawieja SD, Castorena-Gonzalez JA, Scallan JP, Davis MJ. Differences in l-type calcium channel activity partially underlie the regional dichotomy in pumping behavior by murine peripheral and visceral lymphatic vessels. Am J Physiol. 2017
62. Meens MJ, Kutkut I, Rochemont V, Dubrot J, Kaladji FR, Sabine A, Lyons O, Hendrikx S, Bernier-Latmani J, Kiefer F, Smith A, Hugues S, Petrova TV, Kwak BR. Cx47 fine-tunes the handling of serum lipids but is dispensable for lymphatic vascular function. PLoS One. 2017;12:e0181476 [PubMed: 28732089]
63. Scallan JP, Davis MJ. Genetic removal of basal nitric oxide enhances contractile activity in isolated murine collecting lymphatic vessels. J Physiol. 2013;591:2139–2156 [PubMed: 23420659]

64. Davis MJ, Zawieja DC, Gashev AA. Automated measurement of diameter and contraction waves of cannulated lymphatic microvessels. Lymphat Res Biol. 2006;4:3–10 [PubMed: 16569200]

65. Hennig GW. Spatio-temporal mapping and the enteric nervous system. Adv Exp Med Biol. 2016;891:31–42 [PubMed: 27379632]

66. Hennig GW, Gould TW, Koh SD, Corrigan RD, Heredia DJ, Shonnard MC, Smith TK. Use of genetically encoded calcium indicators (gecis) combined with advanced motion tracking techniques to examine the behavior of neurons and glia in the enteric nervous system of the intact murine colon. Front Cell Neurosci. 2015;9:436 [PubMed: 26617487]

67. Hennig GW, Spencer NJ, Jokela-Willis S, Bayguinov PO, Lee HT, Ritchie LA, Ward SM, Smith TK, Sanders KM. Icc-my coordinate smooth muscle electrical and mechanical activity in the murine small intestine. Neurogastroenterol Motil. 2010;22:e138–151 [PubMed: 20059699]

68. Hargens AR, Zweifach BW. Transport between blood and peripheral lymph in intestine. Microvasc Res. 1976;11(1):89–101 [PubMed: 1263867]

69. Benoit JN, Zawieja DC, Goodman AH, Granger HJ. Characterization of intact mesenteric lymphatic pump and its responsiveness to acute edemagenic stress. Am J Physiol. 1989;257:H2059–2069 [PubMed: 2603989]

70. Imtiaz MS, Zhao J, Hosaka K, von der Weid PY, Crowe M, van Helden DF. Pacemaking through ca2+ stores interacting as coupled oscillators via membrane depolarization. Biophys J. 2007;92:3843–3861 [PubMed: 17351003]

71. Souza-Smith FM, Kurtz KM, Breslin JW. Measurement of cytosolic ca2+ in isolated contractile lymphatics. J Vis Exp. 2011

72. Moosmang S, Schulla V, Welling A, Feil R, Feil S, Wegener JW, Hofmann F, Klugbauer N. Dominant role of smooth muscle l-type calcium channel cav1.2 for blood pressure regulation. EMBO J. 2003;22:6027–6034 [PubMed: 14609949]

73. Catterall WA. Voltage-gated calcium channels. Cold Spring Harb Perspect Biol. 2011;3:a003947 [PubMed: 21746798]

74. Dora KA, Doyle MP, Duling BR. Elevation of intracellular calcium in smooth muscle causes endothelial cell generation of no in arterioles. Proc Natl Acad Sci U S A. 1997;94:6529–6534 [PubMed: 9177252]

75. Garland CJ, Bagher P, Powell C, Ye X, Lemmey HAL, Borysova L, Dora KA. Voltage-dependent ca2+ entry into smooth muscle during contraction promotes endothelium-mediated feedback vasodilation in arterioles. Sci Signal. 2017;10

76. Willebrords J, Maes M, Yanguas SC, Vinken M. Inhibitors of connexin and pannexin channels as potential therapeutics. Pharmacol Ther. 2017

77. Coker SJ, Batey AJ, Lightbown ID, Diaz ME, Eisner DA. Effects of mefloquine on cardiac contractility and electrical activity in vivo, in isolated cardiac preparations, and in single ventricular myocytes. Br J Pharmacol. 2000;129:323–330 [PubMed: 10694239]

78. Guan BC, Si JQ, Jiang ZG. Blockade of gap junction coupling by glycyrrhetinic acids in guinea pig cochlear artery: A whole-cell voltage- and current-clamp study. Br J Pharmacol. 2007;151:1049–1060 [PubMed: 17572704]

79. Kim YJ, Elliott AC, Moon SJ, Lee SI, Seo JT. Octanol blocks fluid secretion by inhibition of capacitative calcium entry in rat mandibular salivary acinar cells. Cell Calcium. 1999;25:77–84 [PubMed: 10191962]

80. Connell FC, Ostergaard P, Carver C, Brice G, Williams N, Mansour S, Mortimer PS, Jeffery S, Lymphoedema C. Analysis of the coding regions of vegfr3 and vegfc in milroy disease and other primary lymphoedemas. Hum Genet. 2009;124:625–631 [PubMed: 19002718]

81. Ghalamkarpour A, Morlot S, Raas-Rothschild A, Utkus A, Mulliken JB, Boon LM, Vikkula M. Hereditary lymphedema type i associated with vegfr3 mutation: The first de novo case and atypical presentations. Clin Genet. 2006;70:330–335 [PubMed: 16965327]

82. Irrthum A, Karkkainen MJ, Devriendt K, Alitalo K, Vikkula M. Congenital hereditary lymphedema caused by a mutation that inactivates vegfr3 tyrosine kinase. Am J Hum Genet. 2000;67:295–301 [PubMed: 10856194]

83. Alders M, Hogan BM, Gjini E, Salehi F, Al-Gazali L, Hennekam EA, Holmberg EE, Mannens MM, Mulder MF, Offerhaus GJ, Prescott TE, Schroor EJ, Verheij JB, Witte M, Zwijnenburg PJ,

Vikkula M, Schulte-Merker S, Hennekam RC. Mutations in ccbe1 cause generalized lymph vessel dysplasia in humans. Nat Genet. 2009;41:1272–1274 [PubMed: 19935664]

84. Alders M, Mendola A, Ades L, Al Gazali L, Bellini C, Dallapiccola B, Edery P, Frank U, Hornshuh F, Huisman SA, Jagadeesh S, Kayserili H, Keng WT, Lev D, Prada CE, Sampson JR, Schmidtke J, Shashi V, van Bever Y, Van der Aa N, Verhagen JM, Verheij JB, Vikkula M, Hennekam RC. Evaluation of clinical manifestations in patients with severe lymphedema with and without ccbe1 mutations. Mol Syndromol. 2013;4:107–113 [PubMed: 23653581]
85. Connell F, Kalidas K, Ostergaard P, Brice G, Homfray T, Roberts L, Bunyan DJ, Mitton S, Mansour S, Mortimer P, Jeffery S. Linkage and sequence analysis indicate that ccbe1 is mutated in recessively inherited generalised lymphatic dysplasia. Hum Genet. 2010;127:231–241 [PubMed: 19911200]
86. Shah S, Conlin LK, Gomez L, Aagenaes O, Eiklid K, Knisely AS, Mennuti MT, Matthews RP, Spinner NB, Bull LN. Ccbe1 mutation in two siblings, one manifesting lymphedema-cholestasis syndrome, and the other, fetal hydrops. PLoS One. 2013;8:e75770 [PubMed: 24086631]
87. Bastaki F, Mohamed M, Nair P, Saif F, Tawfiq N, Al-Ali MT, Brandau O, Hamzeh AR. A novel sox18 mutation uncovered in jordanian patient with hypotrichosis-lymphedema-telangiectasia syndrome by whole exome sequencing. Mol Cell Probes. 2016;30:18–21 [PubMed: 26631803]
88. Irrthum A, Devriendt K, Chitayat D, Matthijs G, Glade C, Steijlen PM, Fryns JP, Van Steensel MA, Vikkula M. Mutations in the transcription factor gene sox18 underlie recessive and dominant forms of hypotrichosis-lymphedema-telangiectasia. Am J Hum Genet. 2003;72:1470–1478 [PubMed: 12740761]
89. Petrova TV, Karpanen T, Norrmen C, Mellor R, Tamakoshi T, Finegold D, Ferrell R, Kerjaschki D, Mortimer P, Yla-Herttuala S, Miura N, Alitalo K. Defective valves and abnormal mural cell recruitment underlie lymphatic vascular failure in lymphedema distichiasis. Nat Med. 2004;10:974–981 [PubMed: 15322537]
90. Ivanov KI, Agalarov Y, Valmu L, Samuilova O, Liebl J, Houhou N, Maby-El Hajjami H, Norrmen C, Jaquet M, Miura N, Zangger N, Yla-Herttuala S, Delorenzi M, Petrova TV. Phosphorylation regulates foxc2-mediated transcription in lymphatic endothelial cells. Mol Cell Biol. 2013;33:3749–3761 [PubMed: 23878394]
91. Burrows PE, Gonzalez-Garay ML, Rasmussen JC, Aldrich MB, Guilliod R, Maus EA, Fife CE, Kwon S, Lapinski PE, King PD, Sevick-Muraca EM. Lymphatic abnormalities are associated with rasa1 gene mutations in mouse and man. Proc Natl Acad Sci U S A. 2013;110:8621–8626 [PubMed: 23650393]
92. Fang J, Dagenais SL, Erickson RP, Arlt MF, Glynn MW, Gorski JL, Seaver LH, Glover TW. Mutations in foxc2 (mfh-1), a forkhead family transcription factor, are responsible for the hereditary lymphedema-distichiasis syndrome. Am J Hum Genet. 2000;67:1382–1388 [PubMed: 11078474]
93. Mellor RH, Brice G, Stanton AW, French J, Smith A, Jeffery S, Levick JR, Burnand KG, Mortimer PS, Lymphoedema Research C. Mutations in foxc2 are strongly associated with primary valve failure in veins of the lower limb. Circulation. 2007;115:1912–1920 [PubMed: 17372167]
94. Mellor RH, Tate N, Stanton AW, Hubert C, Makinen T, Smith A, Burnand KG, Jeffery S, Levick JR, Mortimer PS. Mutations in foxc2 in humans (lymphoedema distichiasis syndrome) cause lymphatic dysfunction on dependency. J Vasc Res. 2011;48:397–407 [PubMed: 21464574]
95. Sargent C, Bauer J, Khalil M, Filmore P, Bernas M, Witte M, Pearson MP, Erickson RP. A five generation family with a novel mutation in foxc2 and lymphedema worsening to hydrops in the youngest generation. Am J Med Genet A. 2014;164A:2802–2807 [PubMed: 25252123]
96. Eerola I, Boon LM, Mulliken JB, Burrows PE, Dompmartin A, Watanabe S, Vanwijck R, Vikkula M. Capillary malformation-arteriovenous malformation, a new clinical and genetic disorder caused by rasa1 mutations. Am J Hum Genet. 2003;73:1240–1249 [PubMed: 14639529]
97. Munger SJ, Geng X, Srinivasan RS, Witte MH, Paul DL, Simon AM. Segregated foxc2, nfatc1 and connexin expression at normal developing venous valves, and connexin-specific differences in the valve phenotypes of cx37, cx43, and cx47 knockout mice. Dev Biol. 2016;412:173–190 [PubMed: 26953188]
98. Munger SJ, Kanady JD, Simon AM. Absence of venous valves in mice lacking connexin37. Dev Biol. 2013;373:338–348 [PubMed: 23142761]

99. Kim MS, Gloor GB, Bai D. The distribution and functional properties of pelizaeus-merzbacher-like disease-linked cx47 mutations on cx47/cx47 homotypic and cx47/cx43 heterotypic gap junctions. Biochem J. 2013;452:249–258 [PubMed: 23544880]
100. Orthmann-Murphy JL, Salsano E, Abrams CK, Bizzi A, Uziel G, Freidin MM, Lamantea E, Zeviani M, Scherer SS, Pareyson D. Hereditary spastic paraplegia is a novel phenotype for gja12/gjc2 mutations. Brain. 2009;132:426–438 [PubMed: 19056803]
101. Abrams CK, Scherer SS, Flores-Obando R, Freidin MM, Wong S, Lamantea E, Farina L, Scaioli V, Pareyson D, Salsano E. A new mutation in gjc2 associated with subclinical leukodystrophy. J Neurol. 2014;261:1929–1938 [PubMed: 25059390]
102. Paznekas WA, Boyadjiev SA, Shapiro RE, Daniels O, Wollnik B, Keegan CE, Innis JW, Dinulos MB, Christian C, Hannibal MC, Jabs EW. Connexin 43 (gja1) mutations cause the pleiotropic phenotype of oculodentodigital dysplasia. Am J Hum Genet. 2003;72:408–418 [PubMed: 12457340]
103. Paznekas WA, Karczeski B, Vermeer S, Lowry RB, Delatycki M, Laurence F, Koivisto PA, Van Maldergem L, Boyadjiev SA, Bodurtha JN, Jabs EW. Gja1 mutations, variants, and connexin 43 dysfunction as it relates to the oculodentodigital dysplasia phenotype. Hum Mutat. 2009;30:724–733 [PubMed: 19338053]
104. Scallan JP, Wolpers JH, Davis MJ. Constriction of isolated collecting lymphatic vessels in response to acute increases in downstream pressure. J Physiol. 2013;591:443–459 [PubMed: 23045335]
105. Baliyan V, Tajmir S, Hedgire SS, Ganguli S, Prabhakar AM. Lower extremity venous reflux. Cardiovasc Diagn Ther. 2016;6:533–543 [PubMed: 28123974]
106. Engeset A, Olszewski W, Jaeger PM, Sokolowski J, Theodorsen L. Twenty-four hour variation in flow and composition of leg lymph in normal men. Acta Physiol Scand. 1977;99:140–148 [PubMed: 842370]
107. de Wit C, Hoepfl B, Wolfle SE. Endothelial mediators and communication through vascular gap junctions. Biol Chem. 2006;387:3–9 [PubMed: 16497158]
108. de Wit C, Roos F, Bolz SS, Kirchhoff S, Kruger O, Willecke K, Pohl U. Impaired conduction of vasodilation along arterioles in connexin40-deficient mice. Circ Res. 2000;86:649–655 [PubMed: 10747000]
109. de Wit C, Roos F, Bolz SS, Pohl U. Lack of vascular connexin 40 is associated with hypertension and irregular arteriolar vasomotion. Physiol Genomics. 2003;13:169–177 [PubMed: 12700362]
110. Longden TA, Dabertrand F, Koide M, Gonzales AL, Tykocki NR, Brayden JE, Hill-Eubanks D, Nelson MT. Capillary k+-sensing initiates retrograde hyperpolarization to increase local cerebral blood flow. Nat Neurosci. 2017;20:717–726 [PubMed: 28319610]
111. Garland CJ, Dora KA. Edh: Endothelium-dependent hyperpolarization and microvascular signalling. Acta Physiol (Oxf). 2017;219:152–161 [PubMed: 26752699]
112. Mather S, Dora KA, Sandow SL, Winter P, Garland CJ. Rapid endothelial cell-selective loading of connexin 40 antibody blocks endothelium-derived hyperpolarizing factor dilation in rat small mesenteric arteries. Circ Res. 2005;97:399–407 [PubMed: 16037574]
113. Yu J, Bihari A, Lidington D, Tyml K. Gap junction uncouplers attenuate arteriolar response to distal capillary stimuli. Microvasc Res. 2000;59:162–168 [PubMed: 10625583]
114. Kanady JD, Simon AM. Lymphatic communication: Connexin junction, what's your function? Lymphology. 2011;44:95–102 [PubMed: 22165579]
115. von der Weid PY, Van Helden DF. Functional electrical properties of the endothelium in lymphatic vessels of the guinea-pig mesentery. J Physiol. 1997;504 (Pt 2):439–451 [PubMed: 9365916]
116. Seki A, Ishikawa T, Daumy X, Mishima H, Barc J, Sasaki R, Nishii K, Saito K, Urano M, Ohno S, Otsuki S, Kimoto H, Baruteau AE, Thollet A, Fouchard S, Bonnaud S, Parent P, Shibata Y, Perrin JP, Le Marec H, Hagiwara N, Mercier S, Horie M, Probst V, Yoshiura KI, Redon R, Schott JJ, Makita N. Progressive atrial conduction defects associated with bone malformation caused by a connexin-45 mutation. J Am Coll Cardiol. 2017;70:358–370 [PubMed: 28705318]

117. Frank M, Wirth A, Andrie RP, Kreuzberg MM, Dobrowolski R, Seifert G, Offermanns S, Nickenig G, Willecke K, Schrickel JW. Connexin45 provides optimal atrioventricular nodal conduction in the adult mouse heart. Circ Res. 2012;111:1528–1538 [PubMed: 22982984]
118. Boyett MR, Inada S, Yoo S, Li J, Liu J, Tellez J, Greener ID, Honjo H, Billeter R, Lei M, Zhang H, Efimov IR, Dobrzynski H. Connexins in the sinoatrial and atrioventricular nodes. Adv Cardiol. 2006;42:175–197 [PubMed: 16646591]
119. Yamada KA, Rogers JG, Sundset R, Steinberg TH, Saffitz J. Up-regulation of connexin45 in heart failure. J Cardiovasc Electrophysiol. 2003;14:1205–1212 [PubMed: 14678136]
120. Severs NJ, Dupont E, Thomas N, Kaba R, Rothery S, Jain R, Sharpey K, Fry CH. Alterations in cardiac connexin expression in cardiomyopathies. Adv Cardiol. 2006;42:228–242 [PubMed: 16646594]
121. Kumai M, Nishii K, Nakamura K, Takeda N, Suzuki M, Shibata Y. Loss of connexin45 causes a cushion defect in early cardiogenesis. Development. 2000;127:3501–3512 [PubMed: 10903175]
122. Boardman KC, Swartz MA. Interstitial flow as a guide for lymphangiogenesis. Circ Res. 2003;92:801–808 [PubMed: 12623882]
123. Clavin NW, Avraham T, Fernandez J, Daluvoy SV, Soares MA, Chaudhry A, Mehrara BJ. Tgf-beta1 is a negative regulator of lymphatic regeneration during wound repair. Am J Physiol Heart Circ Physiol. 2008;295:H2113–2127 [PubMed: 18849330]
124. Gousopoulos E, Karaman S, Proulx ST, Leu K, Buschle D, Detmar M. High-fat diet in the absence of obesity does not aggravate surgically induced lymphoedema in mice. Eur Surg Res. 2017;58:180–192 [PubMed: 28301852]
125. Karkkainen MJ, Saaristo A, Jussila L, Karila KA, Lawrence EC, Pajusola K, Bueler H, Eichmann A, Kauppinen R, Kettunen MI, Yla-Herttuala S, Finegold DN, Ferrell RE, Alitalo K. A model for gene therapy of human hereditary lymphedema. Proc Natl Acad Sci U S A. 2001;98:12677–12682 [PubMed: 11592985]
126. Karkkainen MJ, Ferrell RE, Lawrence EC, Kimak MA, Levinson KL, McTigue MA, Alitalo K, Finegold DN. Missense mutations interfere with vegfr-3 signalling in primary lymphoedema. Nat Genet. 2000;25:153–159 [PubMed: 10835628]
127. Bell R, Brice G, Child AH, Murday VA, Mansour S, Sandy CJ, Collin JR, Brady AF, Callen DF, Burnand K, Mortimer P, Jeffery S. Analysis of lymphoedema-distichiasis families for foxc2 mutations reveals small insertions and deletions throughout the gene. Hum Genet. 2001;108:546–551 [PubMed: 11499682]
128. Brice G, Mansour S, Bell R, Collin JR, Child AH, Brady AF, Sarfarazi M, Burnand KG, Jeffery S, Mortimer P, Murday VA. Analysis of the phenotypic abnormalities in lymphoedema-distichiasis syndrome in 74 patients with foxc2 mutations or linkage to 16q24. J Med Genet. 2002;39:478–483 [PubMed: 12114478]
129. Karlsen TV, Reikvam T, Tofteberg A, Nikpey E, Skogstrand T, Wagner M, Tenstad O, Wiig H. Lymphangiogenesis facilitates initial lymph formation and enhances the dendritic cell mobilizing chemokine ccl21 without affecting migration. Arterioscler Thromb Vasc Biol. 2017;37:2128–2135 [PubMed: 28935759]
130. Reed RK, Rubin K, Wiig H, Rodt SA. Blockade of beta 1-integrins in skin causes edema through lowering of interstitial fluid pressure. Circ Res. 1992;71:978–983 [PubMed: 1516168]
131. Emerson GG, Segal SS. Electrical coupling between endothelial cells and smooth muscle cells in hamster feed arteries: Role in vasomotor control. Circ Res. 2000;87:474–479 [PubMed: 10988239]
132. Welsh DG, Segal SS. Endothelial and smooth muscle cell conduction in arterioles controlling blood flow. Am J Physiol. 1998;274:H178–186 [PubMed: 9458866]

Novelty and Significance

What Is Known?

- Patients with inherited mutations in *GJC2* or *GJA1*, encoding gap junction proteins Cx47 and Cx43 respectively, develop primary lymphedema.
- Deficiencies in Cx47, Cx43, and/or Cx37 in mice are associated with developmental lymphatic valve abnormalities; however, similar abnormalities have not been documented in human patients.
- In humans, , defective lymphatic contractile function is proposed to underlie Cx-related lymphedema.

What New Information Does This Article Contribute?

- The major endothelial Cx isoforms – Cx43, Cx47, and Cx37 are dispensable for propulsive, synchronized lymphatic contractions.
- There is functional uncoupling of electrical and Ca^{2+} signals between the lymphatic endothelial and smooth muscle layers that is distinct from the tight coupling found in blood vessels.
- Cx45 is the predominant Cx isoform in the smooth muscle layer of mouse and human lymphatics, and Cx45 mediates the entrainment of electrical and contraction waves in mouse lymphatic smooth muscle.
- Cx45 defects result in impaired lymph transport in the mouse hindlimb only when a gravitational load is imposed, which is consistent with the prevalence of human lymphedema in dependent extremities.
- Cx45 defects potentially lead to lymphedema or exacerbate lymphatic dysfunction in other diseases such as congestive heart failure, obesity, and peripheral artery/venous disease.

Patients with inherited mutations in connexins (Cxs) develop primary lymphedema; however, the underlying reasons are unknown. Possible mechanisms include defects in one-way endothelial valves that minimize lymph backflow or impairment of the spontaneous contractions of lymphatic muscle cells (LMCs), both of which are critical for efficient lymph transport. We find that lymphatic contractions are highly coordinated along lymphatic vessel segments due to the rapid conduction of pacemaking signals between Cx-coupled LMCs. Using transgenic mouse models to delete specific Cx-isoforms, we show that each of the three major endothelial Cxs (Cx47, Cx43, Cx37) are dispensable for the initiation and entrainment of spontaneous lymphatic contractions. We find that smooth muscle-specific Cx45-deficiency results in the disruption of both electrical and contraction waves. Lymph transport is impaired in the intact hindlimbs of Cx45-deficient mice only when a gravitational load is imposed. These findings suggest that lymphedema in the dependent extremities of human patients with Cx47 or Cx43 mutations is related to reduced valve density and/or competency rather than contractile dysfunction or dyssynchrony.

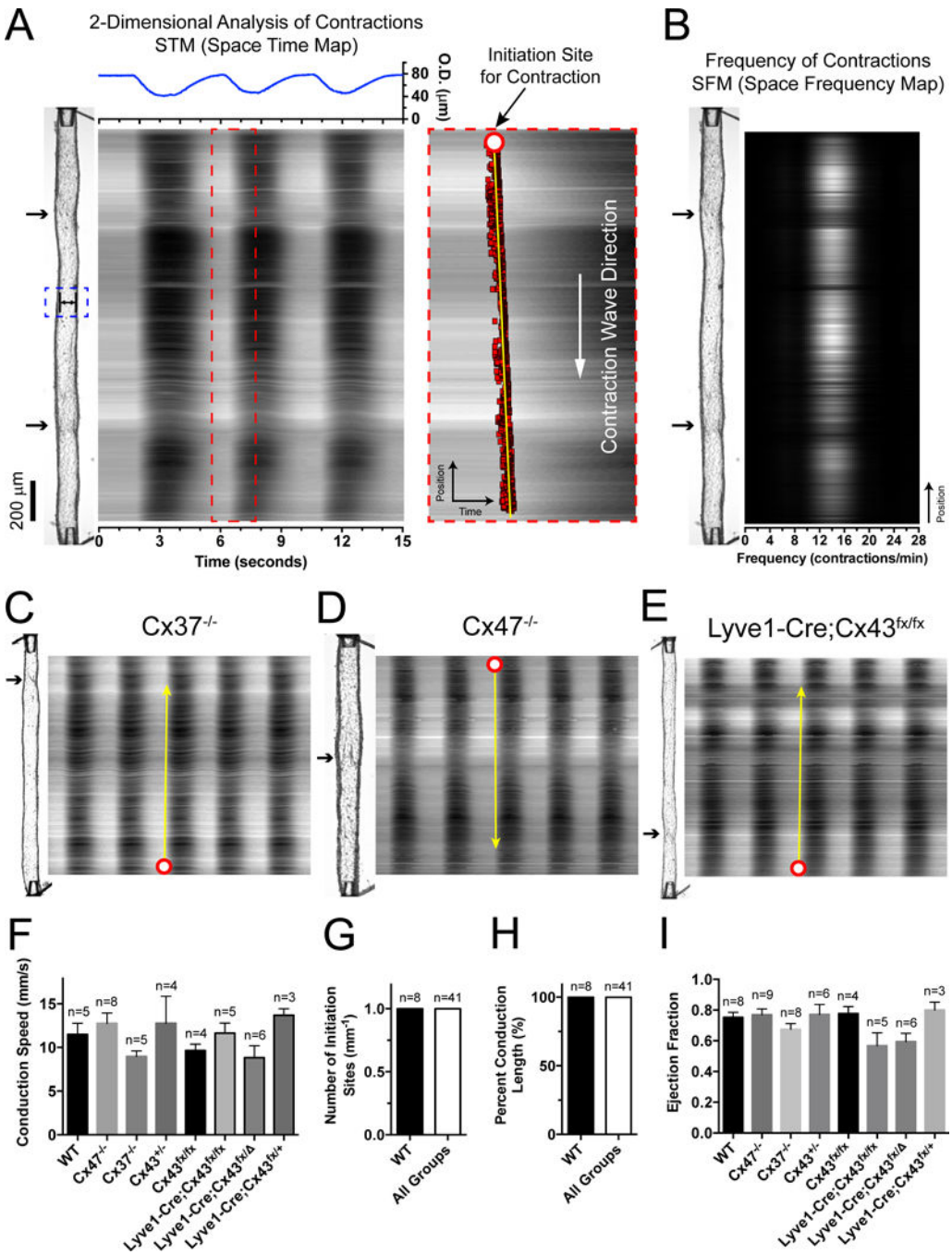

Figure 1. Intercellular coupling through connexins in the endothelial cell layer is dispensable for the generation and coordination of the spontaneous contractions of lymphatic vessels.

(A) A *Space Time Map* (STM) was generated from high-speed, bright-field videos of the spontaneous contractions of a popliteal lymphatic vessel from a WT (*C57BL/6*) mouse; the conduction speed of the propagated contraction wave (see also Online Video I) was measured by edge detection of the wave front at each horizontal pixel followed by a linear fit of the detected points. Red open circle indicates approximate location of the initiation site for the contraction. The top blue trace represents the outside diameter from a single location

specified by the blue dotted box. **(B)** A *Space Frequency Map* (SFM) showing the main contraction frequency components along the lymphatic vessel was generated from a Fourier transform of the corresponding STM. **(C-E)** Representative STMs of entrained, rapidly-conducting spontaneous contractions in popliteal lymphatics from *Cx37*$^{-/-}$, *Cx47*$^{-/-}$ and *Lyve1-Cre;Cx43*$^{fx/fx}$ mice, respectively. Yellow arrows indicate direction of propagation of the contraction waves. Bright-field images of each isolated lymphatic vessel preparation are shown at the left, aligned next to their corresponding STM. Lymphatic valves are indicated with black arrows. **(F-I)** Mean contractile parameters of popliteal lymphatic vessels from control mice and mice deficient in specific endothelial connexin isoforms (i.e. Cx37, Cx43, or Cx47) at 3 cmH_2O intraluminal pressure: conduction speed, number of initiation sites for contractions per unit length, percent conduction length associated with the propagation of contractions, and ejection fraction. No significant differences were found, when comparing all groups and their corresponding controls, using a 1-way ANOVA followed by Dunnett's multiple comparison test with $P<0.05$ (n represents number of animals).

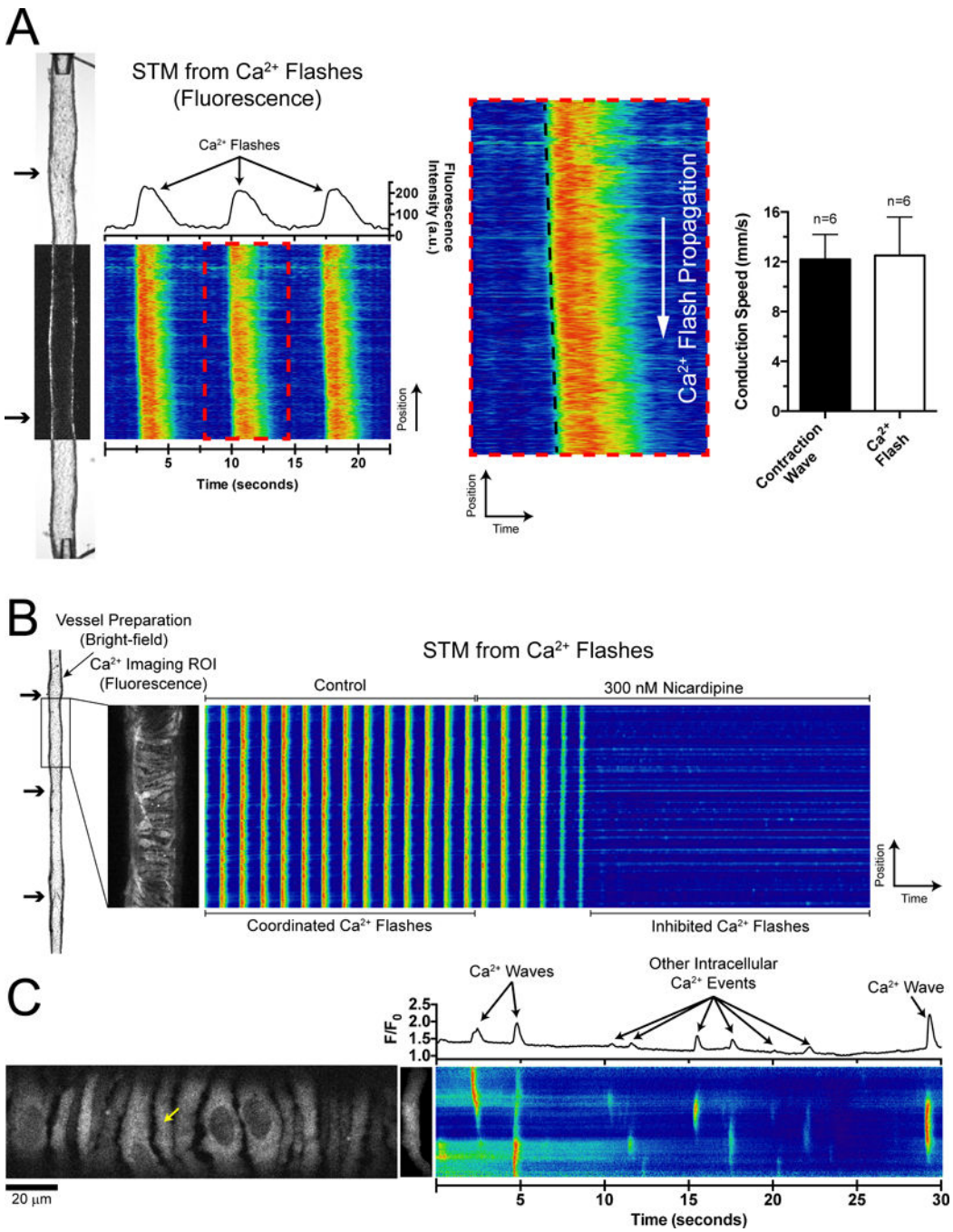

Figure 2. L-type Ca^{2+} channels are essential for the large amplitude, coordinated Ca^{2+} events that precede and drive spontaneous contractions.

(A) A *Space Time Map* (STM) generated from GFP-fluorescence associated with the Ca^{2+} flashes that proceeded contractions in a popliteal lymphatic from a mouse expressing *GCaMP6f* in the muscle layer (*Smmhc-Cre;GCaMP6f*) (see Online Videos II and III). Conduction speed of the Ca^{2+} flash was nearly identical to that of the contraction wave when both were measured in the same vessel segment. **(B)** STM of Ca^{2+} flashes before and after their inhibition by the L-type Ca^{2+} channel blocker nicardipine (300 nM). After

inhibition of Ca^{2+} flashes, various types of underlying intracellular Ca^{2+} events are revealed. **(C)** A single-cell STM showing at least two different types of Ca^{2+} events. See also Online Video IV.

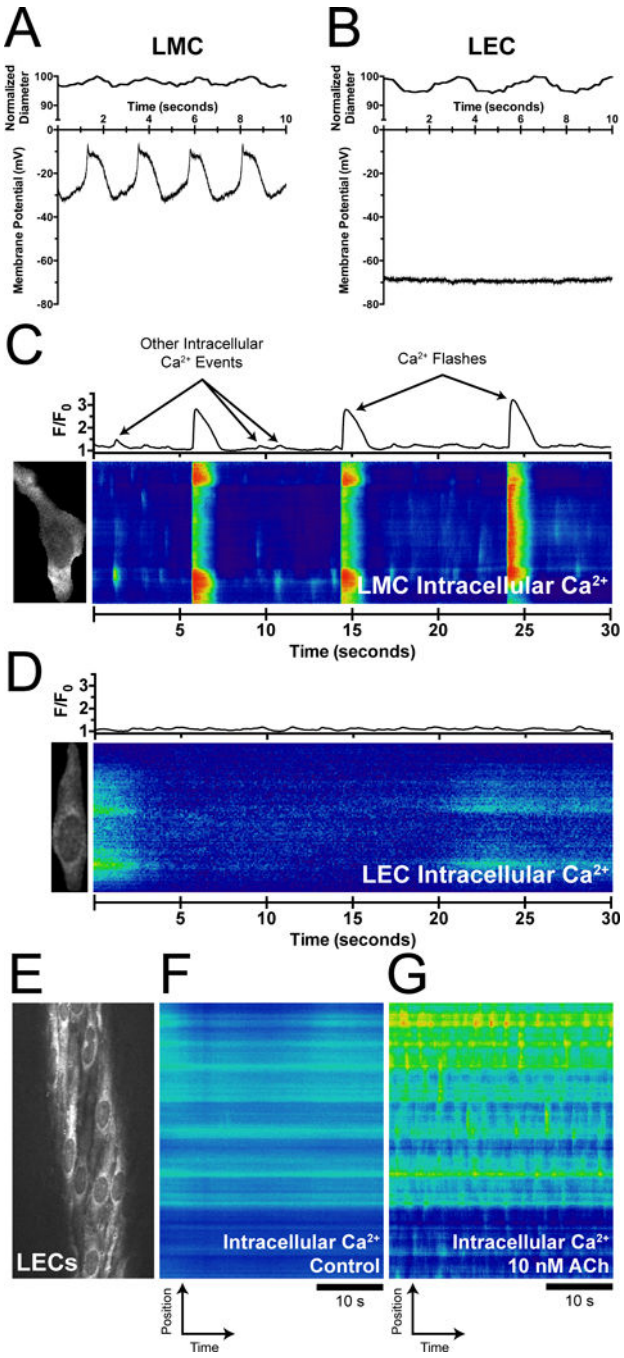

Figure 3. Smooth muscle and endothelial cell layers appear to be uncoupled.

(A-B) Membrane potential recordings from sharp electrodes for a LMC and a LEC, respectively, showing rhythmic firing of action potentials in an LMC but a much more hyperpolarized and quiescent LEC, despite residual contractions in the muscle layer. Contractions were blunted by wortmannin to permit stable V_m recording without dislodging the electrode. **(C-D)** Representative single-cell Ca^{2+} STMs in a LMC and a LEC from popliteal lymphatics from *Smmhc-CreER^{T2};GCaMP6f* and *Prox1-CreER^{T2};GCaMP6f* mice, respectively. LMCs show rhythmic action potentials that trigger the cascade-like influx of

Ca^{2+} (flashes) through L-type Ca^{2+} channels, which drive spontaneous contractions. Ca^{2+} flashes and other intracellular Ca^{2+} events in the LMC layer are not transmitted into the LEC layer. **(E-G)** Endothelium specific intracellular Ca^{2+} events in popliteal lymphatic vessels from *Prox1-CreER^{T2};GCaMP6f* mice. STMs from Ca^{2+} imaging under **(F)** basal conditions, showing very rare spontaneous activity and **(G)** after incubation with 10 nM ACh, which induces Ca^{2+} events in every cell. See also Video V.

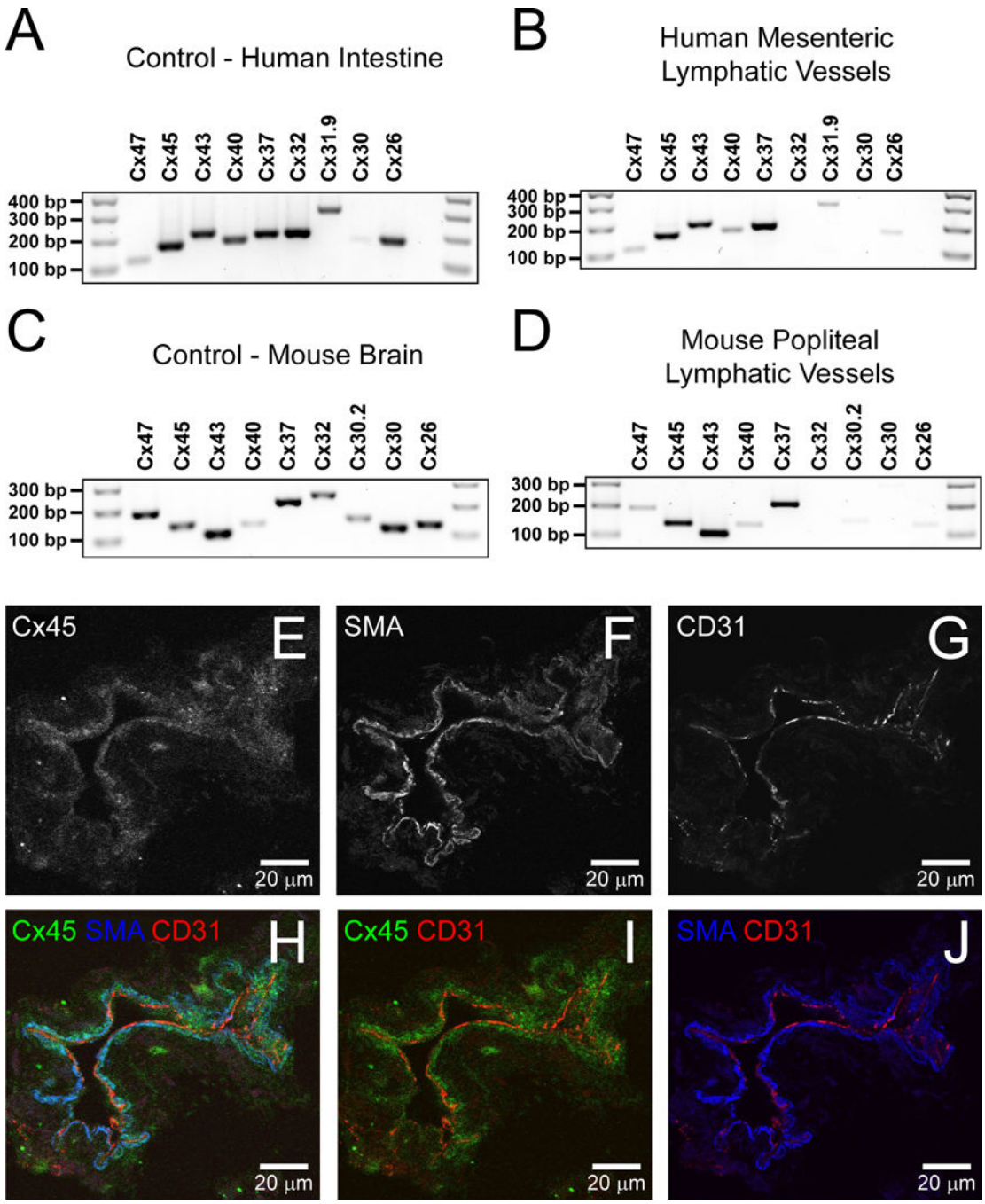

Figure 4. Similar connexin expression in human and mouse lymphatics.

Representative gels showing the mRNA expression for a panel of 9 different vascular connexin isoforms using RT-PCR on intact isolated human mesenteric **(A and B**, n=3**)** and mouse popliteal **(C and D**, n=3**)** lymphatic vessels, as well as their corresponding positive controls (human jejunum wall and mouse brain, respectively). **(E-G)** Immunostaining for Cx45, smooth muscle actin (SMA), and CD31 (PECAM) in transverse sections of mouse popliteal lymphatic vessels. **(H-J)** Cx45 appears to be expressed exclusively in LMCs as evident by its colocalization with SMA but not CD31.

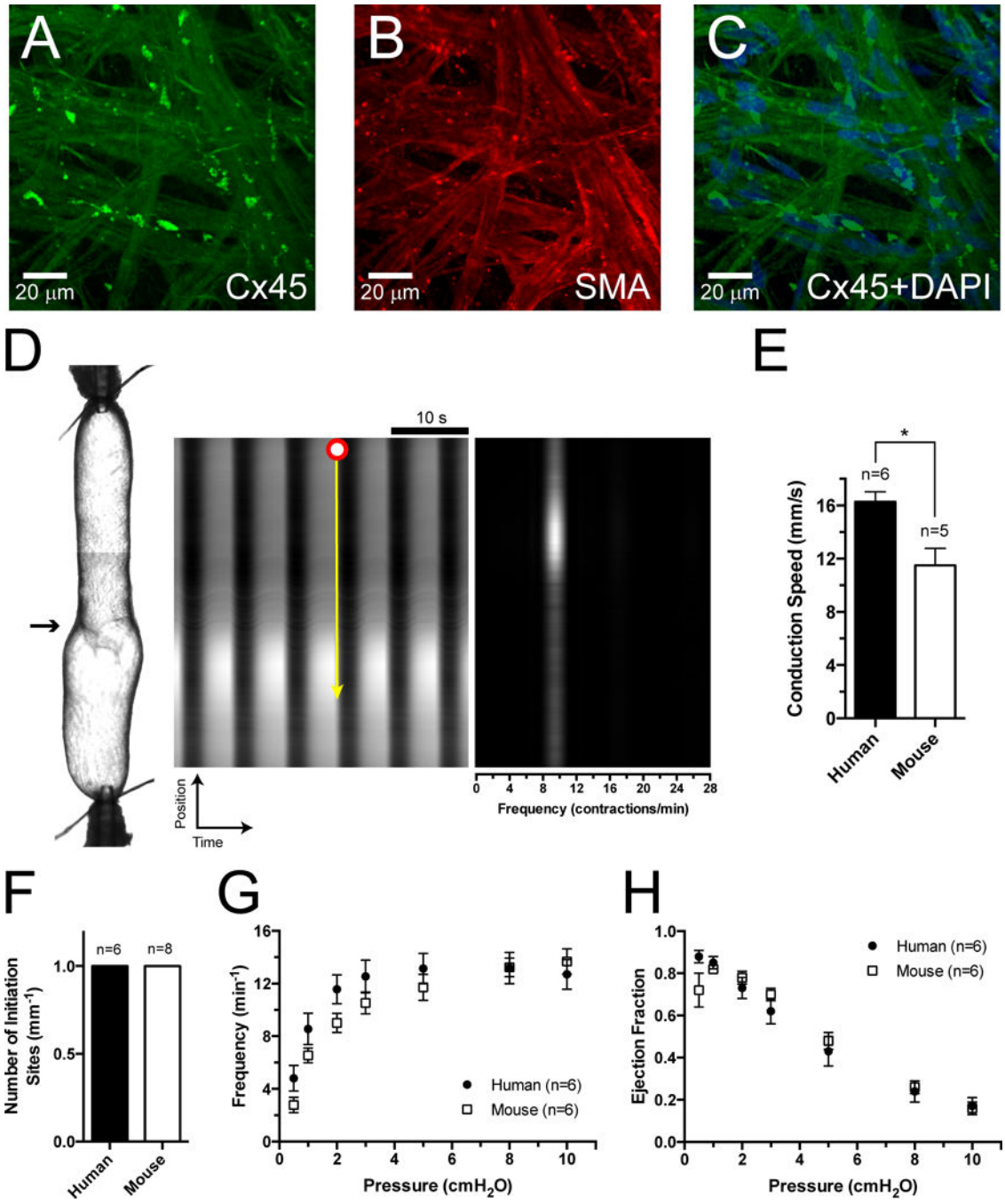

Figure 5. Human mesenteric lymphatics express Cx45 in LMCs and exhibit strong, entrained, rapidly-conducting spontaneous contractions.

(A-C) Immunofluorescence images showing Cx45 expression (co-staining with SMA and DAPI) in the LMC layer of human mesenteric lymphatic vessels (whole-mount). **(D)** Representative STM and SFM (at 3 cmH_2O intraluminal pressure) showing entrained, rapidly-conducting spontaneous contractions of human mesenteric lymphatic vessels (see also Online Video VIII). **(E)** Side-by-side comparison of the mean conduction speed of propagated contraction waves (from bright-field videos of contractions) for human and

mouse lymphatics pressurized to 3 cmH_2O. **(F-H)** Contractile parameters (number of contraction initiation sites, contraction frequency, and ejection fraction) as a function of intraluminal pressure. Significant differences (*) were assessed using 1-way ANOVA followed by Dunnett's multiple comparison test with $P<0.05$ (n represents number of individuals/patients and animals respectively). Additional contractile parameters (i.e. contraction amplitude, tone, end diastolic diameter, and fractional pump flow) are shown in Online Figure VII.

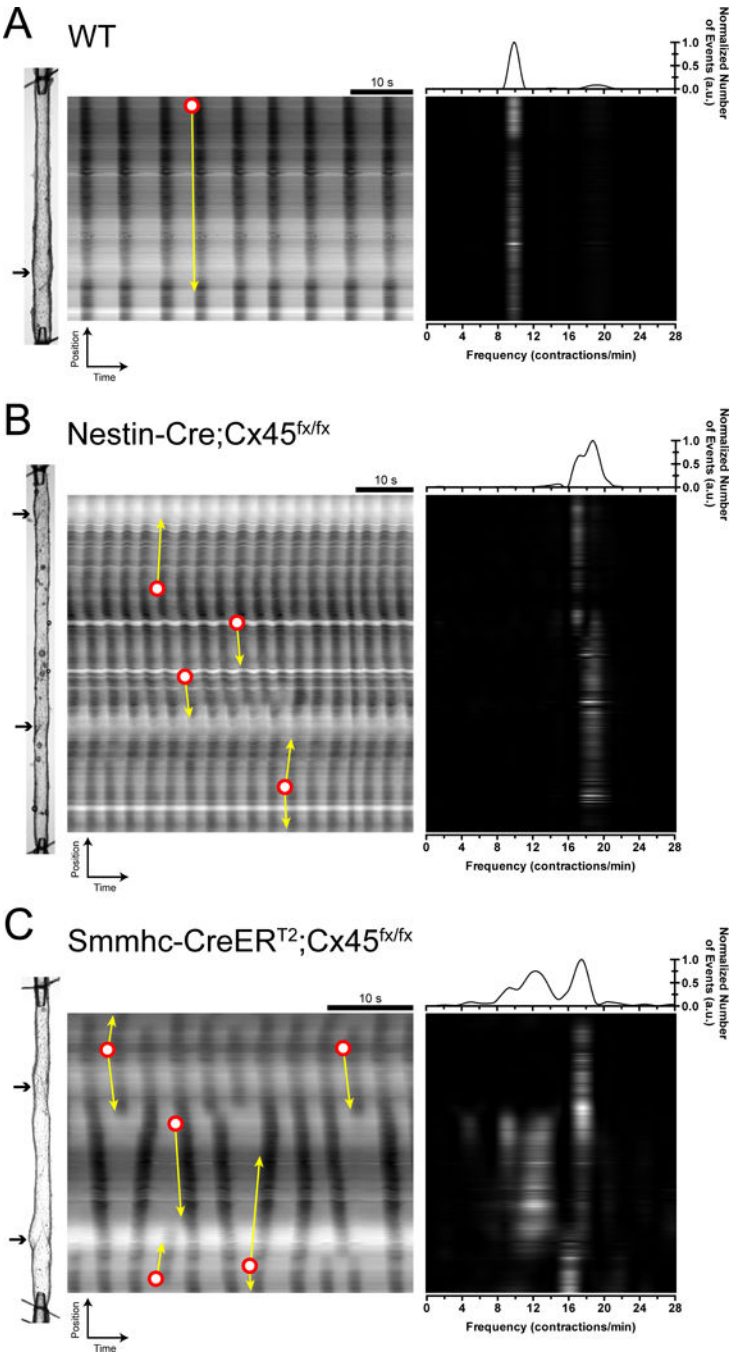

Figure 6. Lymphatic vessels from Cx45-deficient mice exhibit loss of coordination of the spontaneous contractions.

STMs and SFMs showing entrained, rapidly-conducting spontaneous contractions from **(A)** a control (WT) popliteal lymphatic, in contrast to those showing non-coordinated, slowly-conducting, aberrantly-propagating contractions from popliteal lymphatics isolated from **(B and C)** Cx45 deficient mice (*Nestin-Cre;Cx45*$^{fx/fx}$ and *Smmhc-CreER*^{T2}*;Cx45*$^{fx/fx}$, respectively). See also Online Video IX.

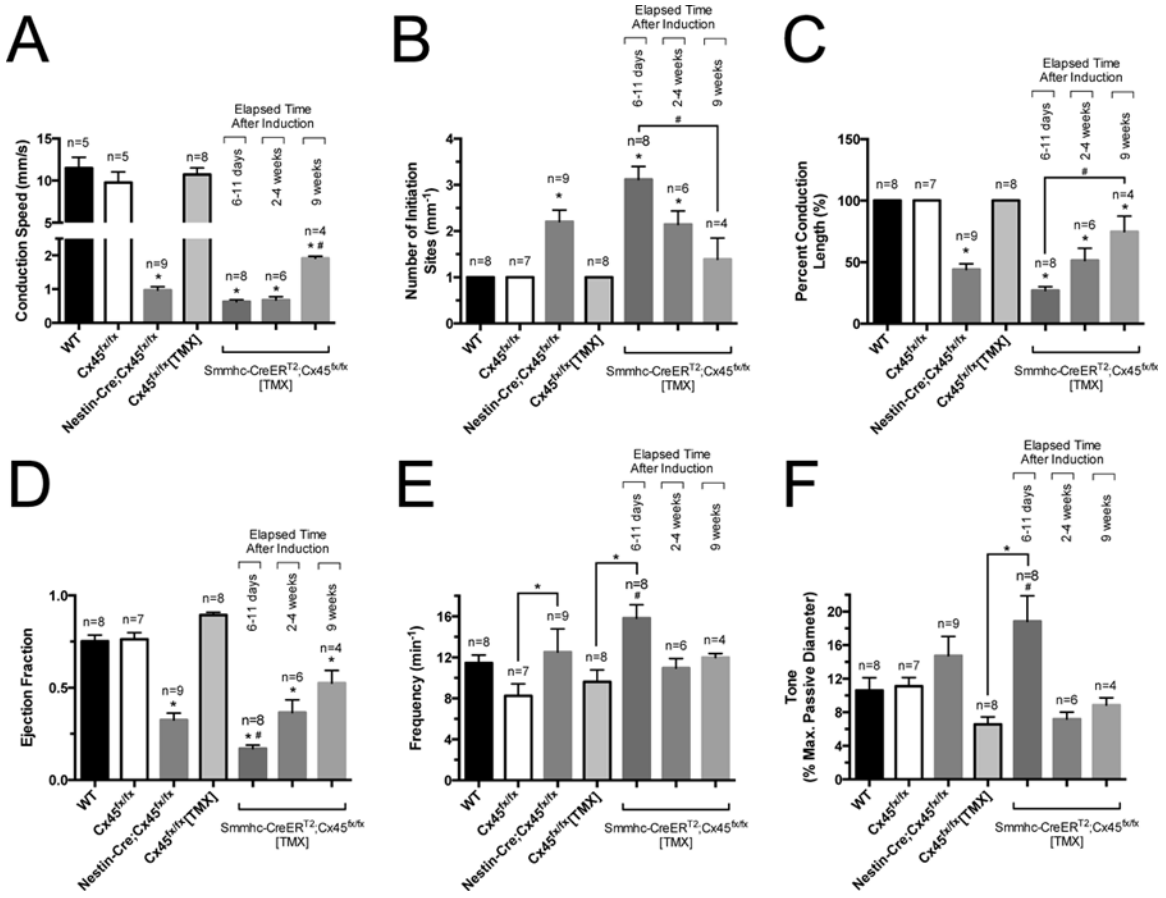

Figure 7. Impaired ejection fraction and slower, aberrantly propagating contraction waves in popliteal lymphatic vessels lacking Cx45 in smooth muscle cells.

(A) Conduction speed, **(B)** number of initiation sites for spontaneous contractions per unit length, and **(C)** percent conduction length associated with the propagation of initiated contractions for popliteal lymphatic vessels from Cx45-deficient mice (*Nestin-Cre;Cx45*$^{fx/fx}$ and *Smmhc-CreER*^{T}*;Cx45*$^{fx/fx}$[TMX](6–11 days post tamoxifen-induction)) and their corresponding controls. The spontaneous contractions of lymphatics from Cx45-deficient mice are uncoordinated, as evident by the increased number of contraction initiation (pacemaking) sites. The impaired electrical coupling between LMCs resulted in a significantly reduced number of LMCs that can be recruited by each pacemaker, leading to: contraction waves with decreased percent conduction length and decreased **(D)** ejection fraction. Electrical coupling between LMCs appears to alter **(E)** contraction frequency and **(F)** tone. These contractile parameters were obtained in vessels pressurized to 3 cmH_2O. Mean values and corresponding SEMs are reported in Online Table I. Significant differences were evaluated at $P<0.05$ using 1-way ANOVA followed by Dunnett's multiple comparison test. The symbol * indicates a significant difference between the specified group(s) and the corresponding direct controls (*Cx45*$^{fx/fx}$ or *Cx45*$^{fx/fx}$[TMX] respectively). When comparing different time-points (6–11 days, 2–4 weeks, and 9-week groups) the symbol # indicates that the specified group was significantly different when compared to a second specified group or groups from all other time-points.

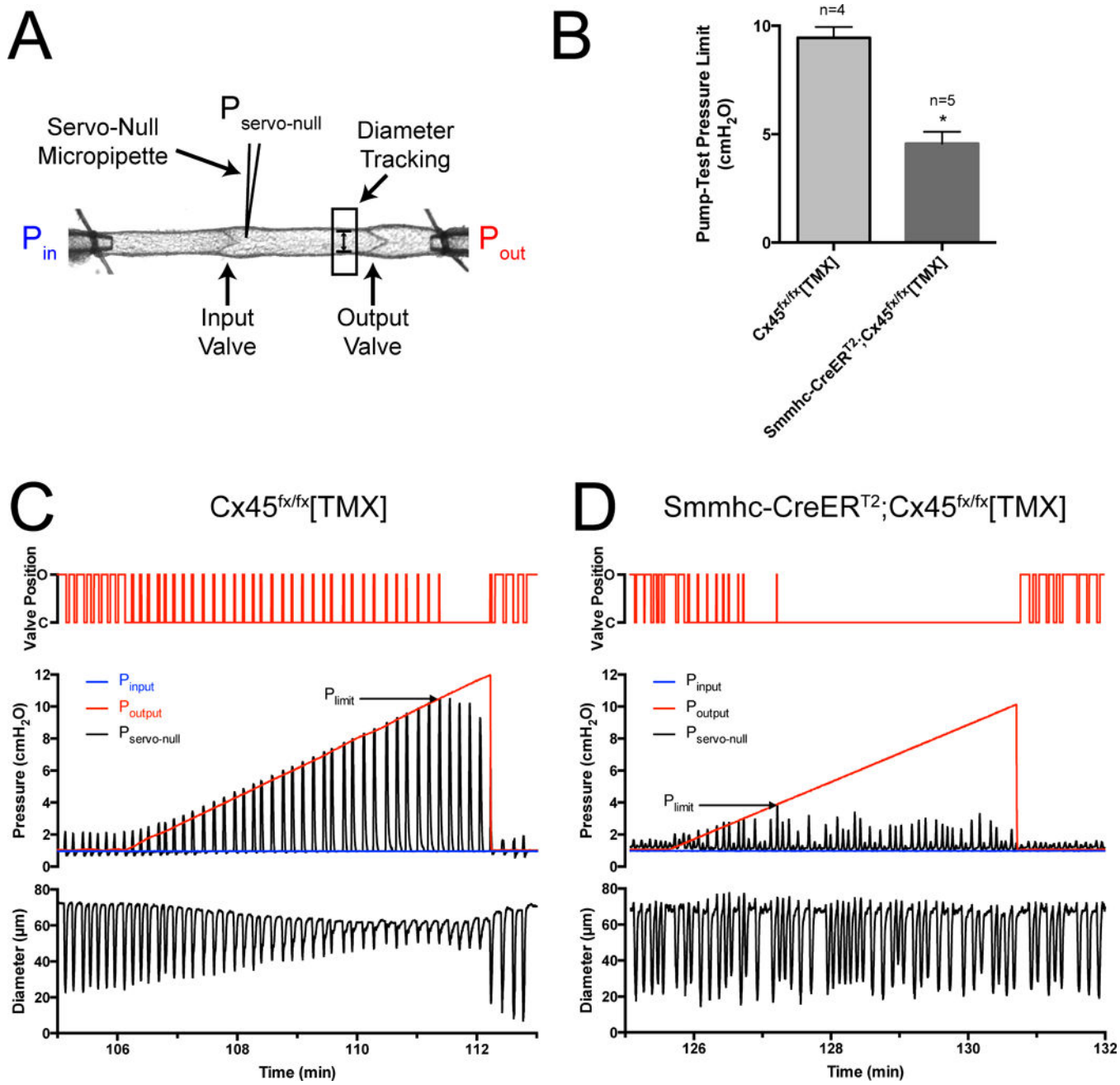

Figure 8. The ability of lymphatic vessels to pump fluid in the presence of an adverse pressure gradient is impaired in vessels from LMC-specific Cx45-deficient mice.

Assessment of the contractile function and lymphatic ability to transport fluid forward when pumping against an adverse pressure gradient in popliteal vessels from control (*Cx45$^{fx/fx}$*[TMX]) and Cx45-deleted (*Smmhc-CreER^{T2};Cx45$^{fx/fx}$*[TMX]) mice. All vessels tested 6–11 days post induction with tamoxifen. **(A)** Diagram of *Pump-Test* preparation (see also Online Video X), **(B)** adverse pressure gradient limit from Pump-Tests (pressure level at which lymphatic vessels failed to open the downstream/output valve), and representative traces (top section: valve opening, middle section: input (blue line), output (red line), and

middle lymphangion intraluminal pressures (black line), and bottom section: tracked luminal diameter) for **(C)** *Cx45*$^{fx/fx}$[TMX] and **(D)** *Smmhc-CreER*^{T2}*;Cx45*$^{fx/fx}$[TMX] respectively.

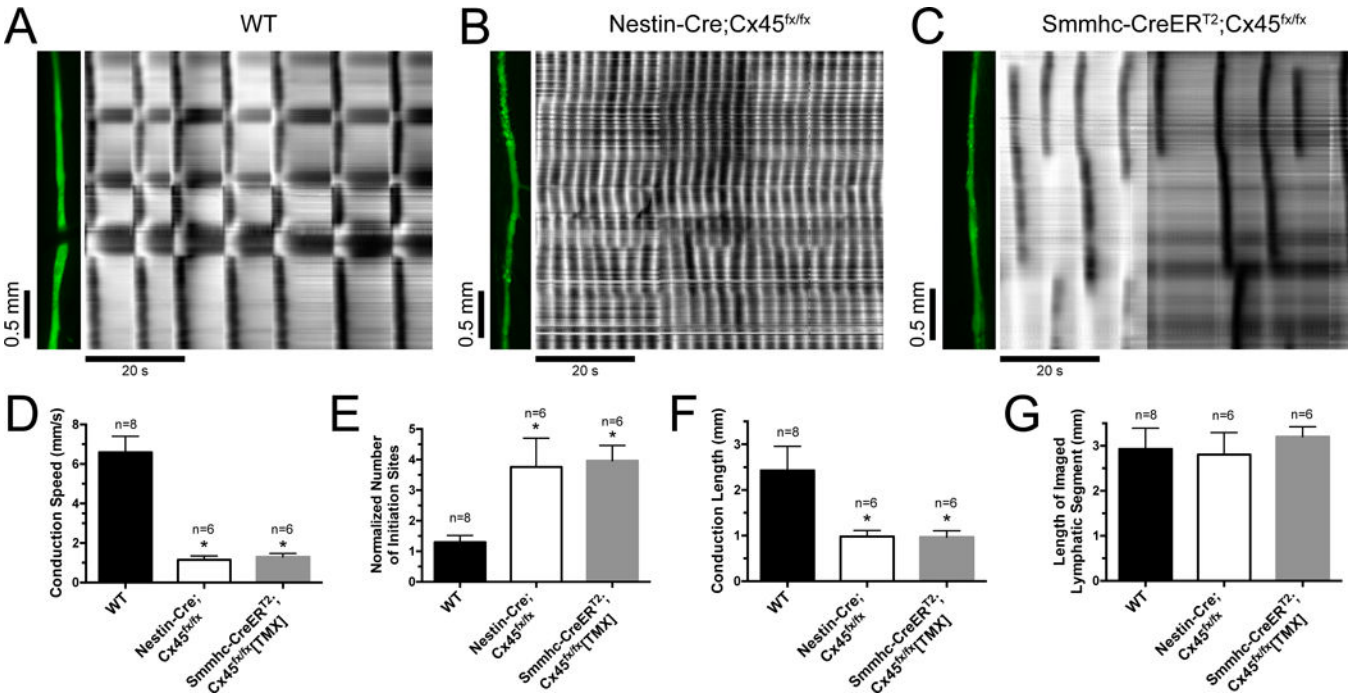

Figure 9. Lack of coordinated spontaneous contractions in popliteal lymphatic vessels in vivo from mice with SMC-specific Cx45 deficiency.

Assessment of the contractile activity of popliteal lymphatic vessels (via fluorescence imaging following FITC-solution injection at the dorsal aspect of the foot) from control and Cx45-deficient (*Nestin-Cre;Cx45*$^{fx/fx}$ and *Smmhc-CreER*^{T2}*;Cx45*$^{fx/fx}$) mice in vivo. STMs of the in vivo contractions of popliteal collecting lymphatics from **(A)** WT, **(B)** *Nestin-Cre;Cx45*$^{fx/fx}$, and **(C)** *Smmhc-CreER*^{T2}*;Cx45*$^{fx/fx}$ mice respectively. In contrast to the rapidly propagating, highly entrained contractions observed in WT mice, contractions of popliteal lymphatics from mice deficient in Cx45 were uncoordinated and slowly propagating. **(D-G)** Conduction speed, normalized number of different initiation sites for contractions, conduction length of propagating contraction waves, and mean length of in vivo imaged popliteal lymphatic segments.

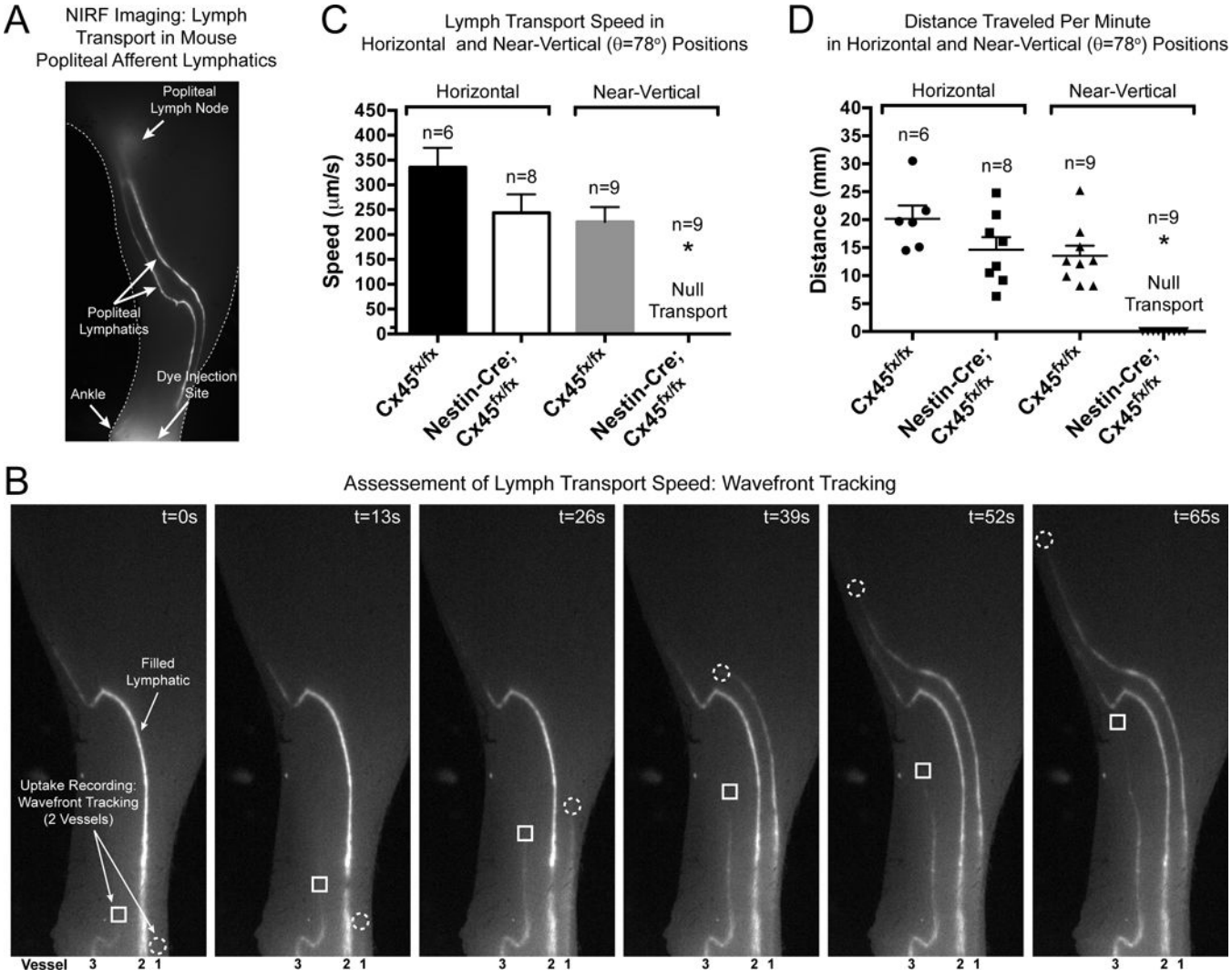

Figure 10. In vivo lymph transport in popliteal lymphatics of SMC-specific Cx45 deficient mice is inhibited when a gravitational hydrostatic load is imposed.

(A) NIRF imaging of (mouse hindlimb) popliteal afferent lymphatics following infrared dye (IRDye® 800CW PEG Contrast Agent) injection in the dorsal aspect of the foot. **(B)** Assessment of lymph transport. Transport speed was determined by tracking the position of the wavefront (at 1 fps) after dye uptake had initiated. Time-lapse images of three vessels (labeled 1–3) are shown in a Cx45-deficient mouse in the horizontal position: in vessels 1 and 3, the wavefront of the dye moving downstream is marked by a dashed-circle or square respectively; vessel 2 filled with dye up to the popliteal node within 2 seconds, at an estimated speed >2 mm/s, indicating it was driven by the pressure head generated by the injection (such vessels were excluded from analysis). **(C)** Mean lymph transport speed and **(D)** normalized distance traveled (per minute) by lymph in popliteal lymphatics from control (*Cx45*$^{fx/fx}$) and Cx45-deficient (*Nestin-Cre;Cx45*$^{fx/fx}$) mice in horizontal and near-vertical (~78^{o}) positions. No significant differences were found in lymph transport between control and Cx45-deficient mice in the horizontal position or in control mice in the near-vertical position. However, lymph transport was completely inhibited in popliteal lymphatics from

SMC-Cx45 deficient mice in the near-vertical position. Significant differences (*) were determined using a 1-way ANOVA followed by Tukey's multiple comparison test (comparing means of all groups) with $P<0.05$ (n represents number of imaged limbs following a single injection with infrared dye). (*) indicates that the *Nestin-Cre;Cx45*$^{fx/fx}$ (in the near-vertical position) group was significantly different from all other groups.